EXTENDED IMMERSION COEFFICIENT SPECTRUM FOR HYPER SPECTRAL RADIOMETERS

by

Nikunjkumar V. Kachhadiya

Submitted in partial fulfilment of the requirements
for the degree of Master of Applied Science

at

Dalhousie University
Halifax, Nova Scotia
October 2018

DEDICATION

To my Parents Vinubhai and Ramaben ,

To my Dear brother Amit, Grandparents and family members,

To my lovely wife, Ripal for her trust and faith in me during this journey.

TABLE OF CONTENTS

LIST OF TABLES

LIST OF FIGURES

ABSTRACT

Satellite mounted with OCI [Ocean Colour Instrument] must be validated and calibrated periodically while commissioned using hyper spectral radiometers. Absolute calibration of Hyper Spectral Radiometers is done in the air in the optical laboratories, and they are deployed in the ocean [Other than air] while calibrating OCI. Sensors response changes compare to air [Lab] while they are operating in the ocean. Calculated calibration coefficients in air must be corrected as sensors response changes due to changes in refractive index of the medium. Two things affect radiance Measurements. First, Sensor's solid angle is reduced in-water compare to in-air and therefore lesser light reaches to the sensor. Second, Refractive index of the medium changes when sensor is submerged in water. Value of RI [refractive index] of the sensor's window is closer to the water value compare to RI of air. Changes in sensors' response is calculated and measured by experiments so called Immersion Factors and then Immersion factors are applied to the calibrated co efficient calculated in the air. As PACE is designed to operate in UV [350-400nm], Visible [400-700nm] and Near Infrared [700-900nm], it is important for HyperNav, a Hyper Spectral Radiometer to obtain Immersion Factors closer to actual values for the full spectrum range.

LIST OF ABBREVIATION USED

HN	HyperNav
Hyper-OCR	Hyper Ocean Colour Radiometer
PACE	Plankton Aerosol Cloud Ocean Eco-System
NASA	National Aeronautics and Space Administration
ARGO	Ship named "ARGO" by which first float was deployed in Ocean
OCI	Ocean Colour Instrument
PM	Particulate Matter
AOD	Aerosol optical Depth
HOA	Harmful Algae Bloom
VIIRS	Visible Infrared Imaging Radiometer Suite
CZCS	Coastal Zone Colour Scanner
SAS	Surface Acquisition System
IC	Immersion Coefficients
APM	Autonomous Profiling Mode
CPM	Continuous Profiling Mode
NIST	National Institute of Standard and Technology
UV	Ultraviolet
IR	Infrared
Si	Silicon
L	Radiance
E	Irradiance

ED	Irradiance Down welling
EU	Irradiance Upwelling
ES	Irradiance Surface
LU	Radiance Upwelling
LI	Radiance Indirect [Sky]
Lt	Radiance total
DN	Digital Number
$DN_p(0^-)$	In Water Measurements
$DN_p(0^+)$	In Air Measurements
C_c	Spectral Calibration Coefficient
L_w	In Water Radiance
L_a	In-Air Radiance
ADC	Analogue to Digital Conversion
HN#x	HyperNav Radiometer,
	Where, # Represents Head No: 1 to 6 & x Presents Experiment
FEL	Free Electron Lamp

ACKNOWLEDGEMENTS

First of all, I would like to thank my Graduate Research Supervisor, Dr. Michael Cada for giving me an opportunity to work and continue my research on Immersion Coefficients. Dr. Cada has guided me from my day one at Dalhousie University and always motivated me to bring out the best from a Graduate Student. Dr. Cada has given me a guidance and motivation to continue my research work at Sea Bird Scientific through ASPIRE Program and encouraged me during my time at Dalhousie University.

Secondly, I would like to express my gratitude to Ronnie Van Dommelen, Keith Brown and Burkhard Plaque from Sea Bird Scientific formerly known as Satlantic LP for giving me guidance throughout this research and providing me valuable inputs and feedback for all the experiments and results.

Furthermore, I would also like to thank my research group "Fiber Optics" for giving me valuable feedback during my group meeting presentations and encouraging me to explore this research area furthermore.

CHAPTER 1 INTRODUCTION

In this Chapter, I have covered the information for the entire big research project from where my research idea was discovered, followed by the research objectives and thesis outline.

1.1 PACE Satellite

PACE [Plankton Aerosol Cloud Ocean Eco-System] is NASA's newest satellite, which is being built to know the health of the current ocean ecosystem and provide the data with their most advanced and next generation Ocean Colour Satellite sensors also known as hyper spectral radiometers [25].

1.1.1 Planktons and Aerosol

Planktons are the live organisms in the ocean, which are responsible for maintaining marine food cycle. They absorb the carbon dioxide and with the help of the sunlight make the food for the other living creature in the ocean [22]. Their bloom and concentration depend on concentration of carbon dioxide, nitrogen, water temperature, salinity of the ocean, nitrogen phosphate, calcium and concentration of chlorophyll.

Aerosols are known as the particle present in the atmosphere, which absorbs and scatters sunlight. They are also represented as a site for chemical reactions where various toxic gases in atmosphere react with these particles. There are basically their types of aerosols present in the atmosphere. Human made Aerosol, Dessert dust particles and Volcanic Aerosols. It is important to know what kind of aerosols are present in different parts of the world as they are mainly responsible for what type of clouds will be formed, what kind of rain will be there in particular area and also what amount of sunlight will reach to ground.

1.1.2 History

What is PACE [Plankton Aerosol Cloud Ocean Eco-System]? PACE is NASA's satellite equipped with next generation of Ocean Colour Sensors. In 1978 NASA have launched their first to observe chlorophyll named as CZCS [Coastal Zone Colour Scanner]. CZCS was equipped with multi-spectral radiometer and was capable of collecting data a certain specific wavelength only [12].

In 2011, VIIRS [Visible Infrared Imaging Radiometer Suite] was launched to observe ocean colour, Land, aerosol and cloud research. New Radiometers were added on in the following years to maximize the measurements at multiple wavelengths over the spectrum.

PACE will be launched in 2022, which will be equipped with Hyper Spectral Ocean colour Radiometers, capable of taking measurements at <5nm over the spectrum. PACE will collect data for UV [350-400nm], Visible [400-700nm] and Near Infrared [700-900nm].

1.1.3 Applications

- **Air Quality:** It is measured in PM [Particulate matter concentration] and sometimes it is also predicted from AOD [Aerosol optical Depth]. It is important to know the PM of the particular area/country as it affects the health of the humans living that area [25].

- **Fisheries:** Based on the satellite images from PACE and ocean colour, NASA will be able to predict the fish concentration in particular oceans. It will directly benefit the NOAA and Local fishermen [25].

- **Harmful Algae Bloom:** Harmful Algae Bloom can kill fish and create imbalance in the ocean eco system. It has to be monitored for healthy ocean eco system. With PACE satellite, we will be able to observe algae bloom in various oceans [25].

- **Improving Hazard Assessments and Aviation Safety:** Aviation operations depend on aerosol present in the atmosphere [25]. With Volcanic plums it can be affected. PACE will provide the knowledge, amount, location of the volcanic ash and other harmful aerosol, which can be helpful in Aviation Safety.

1.2 Argo Float Map

As these Satellites provides images and data for the Earth and Ocean. They need routine maintenance and calibration, which can be done remotely through floats in the Ocean. ARGO Floats are currently having a network of close to 4000 floats across the world, which are monitored by ARGO. Not all of the floats are used for Satellite calibrations. Most of them are used to monitor fishing activities; salinity and temp of the ocean, or to predict weather and seasons by local governments. First float was deployed in ocean in 2000 and from then every year hundreds of new floats are added.

At Satlantic, I was working on a research project to design one of these floats to calibrate PACE satellite, which is scheduled to launch in 2022.

1.3 Research Objective

While designing an instrument in the lab it is very important to calibrate the instrument to maintain the instrument accuracy. Calibration process is a technique used by the industry to operate the instrument for the best results with given parameters within acceptable Range.

Radiometers are usually calibrated in the lab in air and then they are used in another medium, more often in the water. Instruments response changes when they are deployed in the different medium other than they are calibrated in. Most of the time theoretical data is used to correct the radiometric data after the data is collected in operating medium. Immersion coefficients are one of the main correction parameters applied on the instruments radiometric data.

Research objective were:

1. To calculate and measure the practical immersion coefficients in operating medium, which can be simultaneously applied to the radiometric data of the radiometers while data is being collected.
2. To extend the range for practically obtained immersion coefficients from 300-900nm to match the PACE's wavelengths in Ultraviolet and near infrared regions.

1.4 Thesis Outline

In First chapter thesis objective is described as a part of a big research project, PACE [Plankton Aerosol Cloud Ocean Eco-System]. In Second chapter Background, Motivation and History is described. Design of the Radiometer is also described alongside with the various radiometers at Satlantic used in the research to collect and analyze data. In Third Chapter theoretical and practical approaches are shown to calculate and measure the data. In Fourth Chapter series of experiments are shown and analysis is also shown after each experiment. All the modifications are described as they were done after each experiment. Final chapter summarised the conclusion and possible future work for this research.

CHAPTER 2 BACKGROUND

In this chapter, I have described different terminologies used in spectroscopy and in ocean science to better understand Immersion effect, Immersion coefficients and its effect on radiometric data. Classification of various Radiometers is also described in this chapter. Some of these radiometers were used in field experiments to obtain the research objective.

2.1 Radiometers

Radiometer is a device used to measure the radiant energy from a source ranging from Ultraviolet to Infrared regions. There are two ways to collect the light, Radiance [From Certain angle] or Irradiance [From all angles]. Spectrometer is often described as a device used to process the light measured by the radiometer. Spectrometers are not a full system and that's why they need to combine with Radiometers often known as Spectroradiometer [12]. They are a complete independent system and can be used without using PC as they have on board processing mechanism.

Radiometers have mainly two parts. It has an optical system which collects the radiance/irradiance energy form a source/object through an aperture and disperse it through filters and finally focus on a field stop also known at detector. A detector converts this radiant energy into Analogue Electrical Signal. In Spectroradiometer there is also a third component which converts Analogue signal to Digital counts, which can be measured and plotted.

2.2 Spectral Resolution

Spectroradiometer is device used to measure the light emitted from the light source. Spectral resolution defines the characteristics of the Spectroradiometer, which can be also described as the channel width in the given bandwidth. Higher the channel gap lesser the spectral resolution and vice versa. Spectral resolution is the factor used to distinguish between Multispectral and Hyper Spectral Radiometers. A sensor will have lower spectral resolution if it has lesser number of bands capable of taking measurements in given bandwidth.

Low Spectral Resolution means a large band with all the information located in one channel over the full bandwidth. Whereas high spectral resolution means a large band divided into multiple channels where each band has information [10].

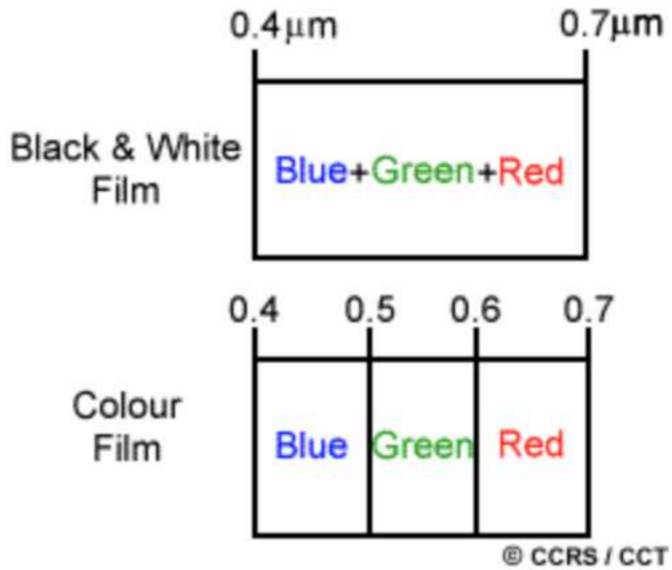

Figure 1 Difference between low spectral resolution and high spectral resolution. Image by Canada Centre for Remote Sensing [https://www.nrcan.gc.ca/earth-sciences/geomatics/satellite-imagery-air-photos/satellite-imagery-products/ educational-resources/9393]

More often Spectroradiometer is classified in to two categories.

- Multispectral Radiometers
- Hyper-Spectral Radiometers.

Multispectral Radiometers has usually less than 20 bands in the full bandwidth. And Hyper-Spectral Radiometers has more than 20 bands in the full bandwidth. In the Figure below Difference between Multispectral and Hyper-Spectral Radiometers are shown.

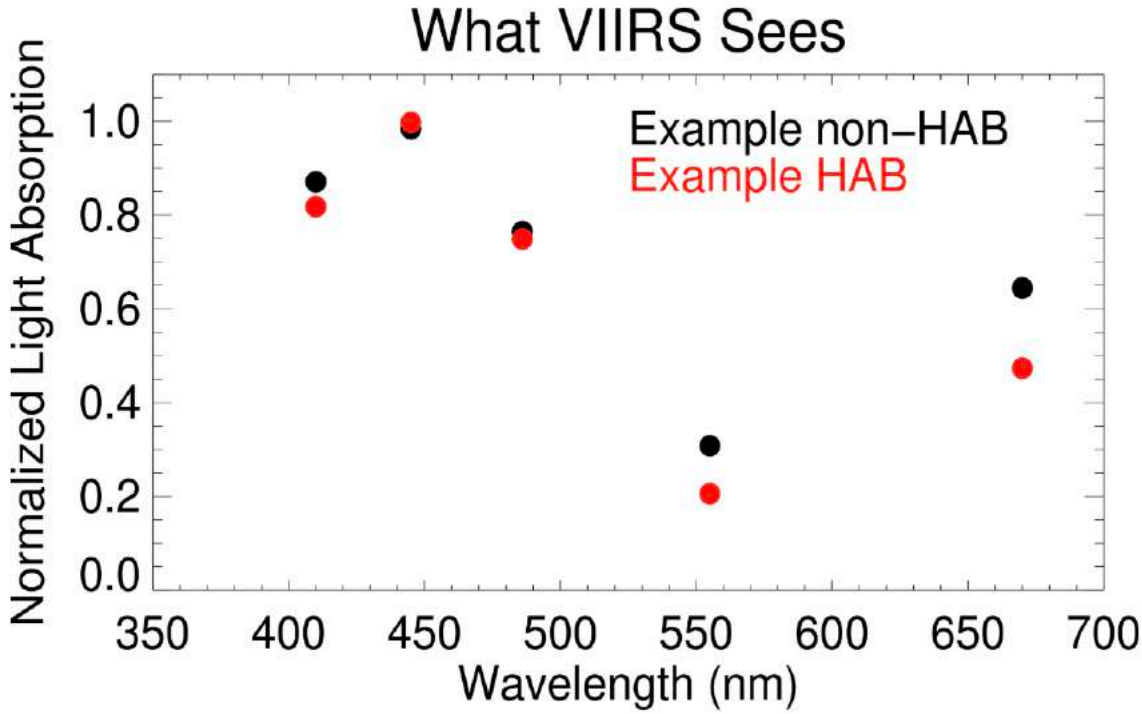

Figure 2 VIIRS [Visible Infrared Imaging Radiometer Suite] is NASA's current ocean colour observing satellite, which has multispectral OCI, collecting data at five wavelengths in a bandwidth [350-700nm]. Image by NASA From [https://pace.oceansciences.org/]

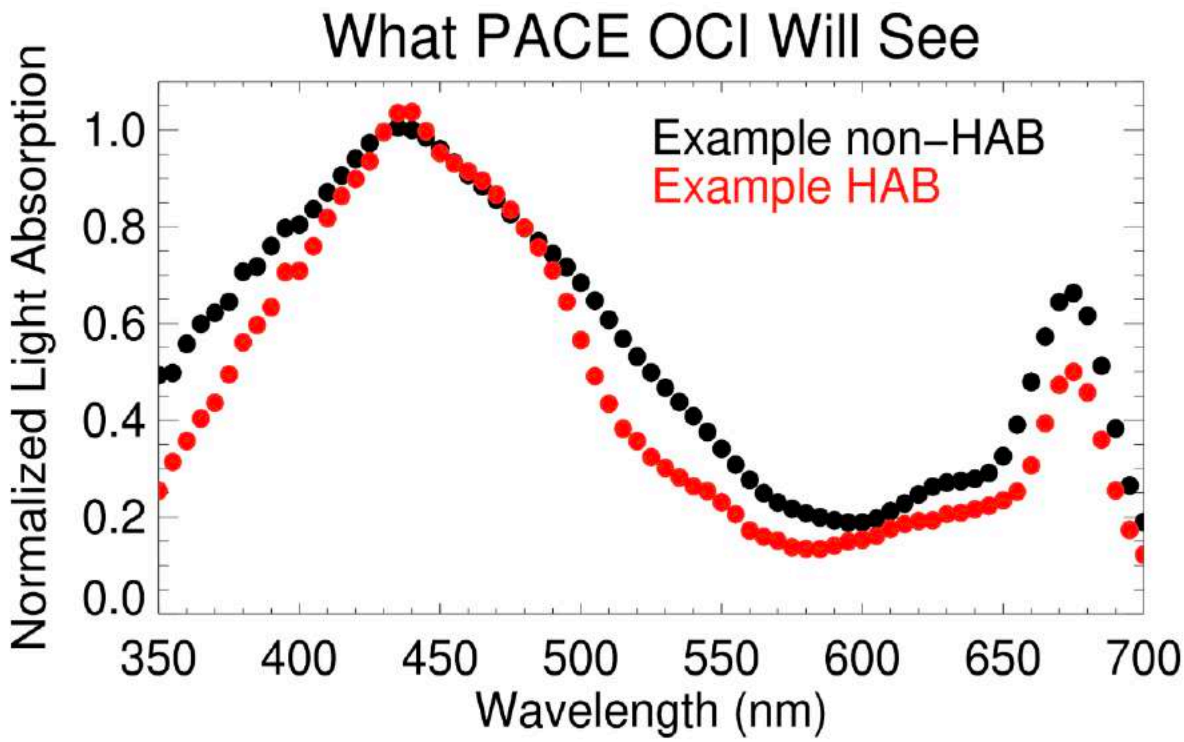

Figure 3 PACE [Plankton Aerosol Cloud Ocean Eco-System], a satellite which is about to launch in 2022 will have a hyper-spectral OCI, collecting data at 5 nm. Image by NASA From [https://pace.oceansciences.org/]

2.3 Radiance and Irradiance Sensors

Energy can be measured in two ways. It is Either Radiance or Irradiance. Radiant energy is defined as energy radiated from the light source and which can be measured at certain angle [5]. Sensor, which is built to measure radiance energy, is often known as Radiance Sensor. Radiance is measure of the energy or power emitted per unit area by the surface at specified angle [20]. Radiance of the sensor is measured in W S_r^{-1} m^{-2} denoted by L. Irradiance is measure of the energy or power received per unit surface area denoted by E. Irradiance of the sensor is measured in W m^{-2}.

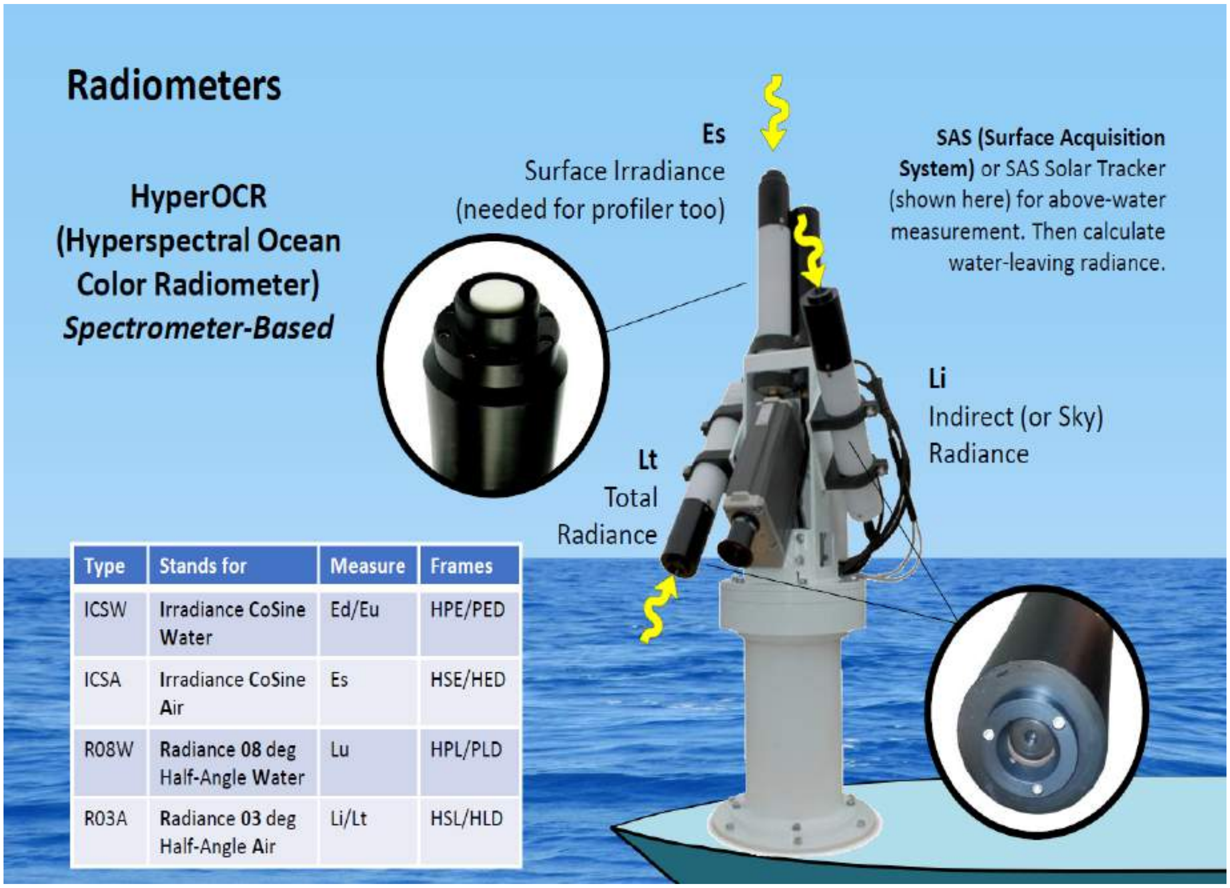

Figure 4 SAS [Surface Acquisition System] is shown with Radiance and Irradiance sensors. This device is one type of Hyper-OCR, which is used to calculate water-leaving radiance. [Ronnie Van Dommelen, Satlantic Inc.]

In the Figure above, SAS system is shown which is a combination of Radiance and Irradiance sensors to collect data for above water measurements. Surface Irradiance sensor Es, mounted on the top measure's sunlight from every direction, which will work as a reference sensor while collecting the Spectral Radiance. Another Radiance sensor is mounted on it, Li, will also work as reference radiance sensor.

Total Radiance Sensor, Lt will collect light coming from the ocean. As sunlight penetrates through ocean, most of it will get absorbed while some of it will get reflected. Radiance Sensor measures reflected light.

Figure 5 Hyper-Pro Profiler is shown in the Figure which is used to collect data below surface. [Ronnie Van Dommelen, Satlantic Inc.]

Hyper-Pro Profiler is a device used to collect light from the ocean floor, which can be used to better understand the ocean's eco-system. Which consist of Ed, Downwelling Irradiance and Lu, Upwelling Radiance sensor.

2.4 HyperNav Spectroradiometer

HyperNav is the System going to be used as Calibration system for PACE [Plankton Aerosol Cloud Ocean Eco-System] Satellite for 2022 [25]. It Consist of Pressure Sensor, Temperature Sensor, Tilt Sensor and Compass as well as two spectrometers and Hardware to process data onboard.

HyperNav Spectroradiometer has 2048 channels in the spectrum ranging from 180nm to 1080nm, which makes channel length less than 1nm. PACE will collect data for UV [350-400nm], Visible [400-700nm] and Near Infrared [700-900nm] [25]. PACE is operating from 350-900 nm range, which will make HyperNav most sophisticated device to calibrate NASA's Next generation satellite.

HyperNav is capable of taking measurements at 1000m below sea level as well as transferring the collected data to satellite when it ascends to surface using Modem.

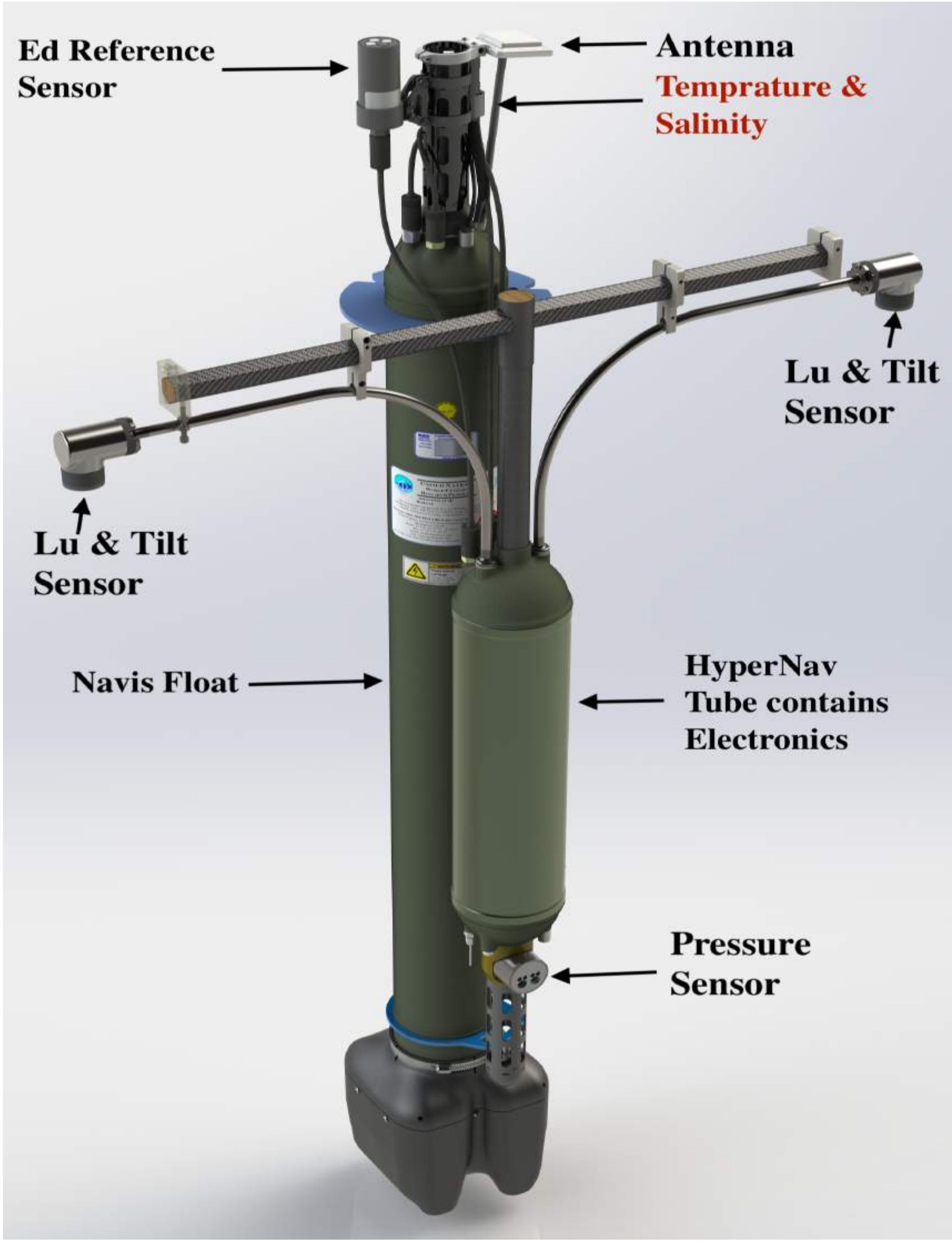

Figure 6 HyperNav Spectroradiometer with Tilt sensor, Temperature sensor; pressure sensor and Reference Radiance Sensor [OCR 504] mounted on Navis Float.

HyperNav is designed and tested for

- Immersion
- Linearity
- Stray Light
- Thermal effects

2.4.1 Operation

HyperNav is designed to operate in Ocean. Using the boat, HyperNav is deployed in the ocean with the NAVIS float. NAVIS Float has Batteries and weights, which is capable of taking HyperNav at 1000m depths in the ocean. When it reaches required depth, HyperNav ascends to the surface slowly as programmed in the on-board electronics taking the measurements at certain depth values.

When it comes closer to the surface, it takes continuous measurements. And it is counted as one profile. Once profile is completed NAVIS program handover control to onboard antenna to transfer this profile to satellite to match the Data. When Data Transfer is complete, NAVIS descends the whole system into the ocean at maximum possible depth and stays there until next profile. By keeping HyperNav at the maximum depth of the ocean it prevents system from Bio fouling. Bio fouling [33] is the term used in ocean science, which refers to microbial biofilms on the surface of the systems in the ocean, which can damage the system over the period of the time.

2.5 Immersion

Radiometers are usually calibrated in the Air and then they are used in other medium than air [e.g. Water]. Instrument's response changes due to changes in the refractive index of the medium. Difference between in-air and in-water response of the radiometers is described by Immersion effect and measured by the immersion co efficient. Change in Response of the instrument is a necessary factor to measure and calculated for as it adds uncertainty to the measured data [29]. Immersion effects were first observed and studied by Atkins and Poole [2] in 1933. They did the experiment to describe the internal reflection factors and external reflection factors when instrument is submerged in to water. Air-Glass and Water Glass refractive indices were taken into measurements and they have concluded the immersion factor 1.09 at end of the experiment.

CHAPTER 3 THEORY AND APPROACH

Now we know the immersion effect, immersion co efficient and its significance in radiometry, I have covered theatrical calculations for the immersion co efficient in this Chapter and also in the end setup of experiment and calculations are covered.

Absolute calibration of Hyper Spectral Radiometers is done in the air in the optical laboratories, and they are deployed in the ocean [Other than air] while calibrating OCI. Sensors response changes compare to air [Lab] while they are operating in the ocean. Calculated calibration coefficients in air must be corrected as sensors response changes due to changes in refractive index of the medium [28] [32]. Two things affect radiance Measurements. First, Sensor's solid angle is reduced in-water compare to in-air and therefore lesser light reaches to the sensor. Second, Refractive index of the medium changes when sensor is submerged in water. Value of RI [refractive index] of the sensor's window is closer to the water value compare to RI of air. Changes in sensors' response is calculated and measured by experiments so called Immersion Factors and then Immersion factors are applied to the calibrated co efficient calculated in the air.

3.1 Theoretical Calculations

Effect of Immersion Factors has been first calculated and observed in 1930's by Atkins and Poole [2]. Westlake 1965 [26], Aas & Smith 1969 [1] [21], Austin 1976 [3] and Zibordi 2004 and 2005 [29] [30] carried further research and development forward. Various measurements techniques and Theoretical models were analysed and proposed by Smith 1969 [21], Muller and Austin 1995 [16] and following revisions in 2003 [15], which were adopted by Ocean science community as standard. Zibordi have made changes in measurements technique the proposed model in 2004 and subsequent changes in 2006 [29] [31].

Spectral Radiance power of any given sensor is given by [31];

$$\emptyset_m = L_m A \Psi_m t_{mg} T_o \tag{1}$$

Where; $\emptyset_m$ represents Spectral Radiance Power, L_m is Radiance detected in the medium with refractive index of n_m, A represents Active surface of detector, Ψ_m is Viewing angle defined by sensor half field of view denoted by θ_m. t_{mg} represents Transmittance of the sensor's window with intervening medium. T_o defined as Transmittance of the other optical components.

Spectral Radiance Power is also described as (Zissis 1993) [27];

$$\emptyset_m = \frac{DN_m}{R_\emptyset} \tag{2}$$

Where DN_m is Spectral Radiance measured by Radiometer and $R_\emptyset$ is Spectral responsivity of the Radiometer detector.

Eq. (1) and Eq. (2) should be written for two mediums using notations a for air and w for water.

$$\emptyset_a = L_a A \Psi_a t_{ag} T_o \tag{3}$$

$$\emptyset_w = L_w A \Psi_w t_{wg} T_o \tag{4}$$

$$\emptyset_a = \frac{DN_a}{R_\emptyset} \tag{5}$$

$$\emptyset_w = \frac{DN_w}{R_\emptyset} \tag{6}$$

By Comparing ratio's of Eq. (3) & (4) and (5) & (6),

$$\frac{\emptyset_a}{\emptyset_w} = \frac{DN_a}{DN_w} = \frac{L_a A \Psi_a t_{ag} T_o}{L_w A \Psi_w t_{wg} T_o}$$

$$L_w = L_a \frac{\Psi_a t_{ag} DN_w}{\Psi_w t_{wg} DN_a} \tag{7}$$

Spectral Radiance of any given sensor looking at light source is directly dependant on radiometric measurements in any given medium [31] denoted as L_m;

$$L_m \propto DN_m$$

$$L_m = C_c I_{f_m} DN_m \tag{8}$$

Where C_c is Spectral Calibration co efficient calculated in the lab through experiments. I_{f_m} represents Spectral Immersion factor calculated based on theory and refractive indices of mediums and Glass window material.

Using a for air and w for water, Eq. (8) can be written as

$$L_w = L_a \frac{DN_w I_{f_w}}{DN_a} \tag{9}$$

By Comparing Eq. (7) and Eq. (9) Immersion Factor I_{f_w} is given as;

$$I_{f_w} = \frac{\Psi_a t_{ag}}{\Psi_w t_{wg}} \tag{10}$$

Where I_{f_w} represents Spectral Immersion Factor in given medium [Water in our case]. $\frac{\Psi_a}{\Psi_w}$ is change in sensor's field of view when it is submerged into water. $\frac{t_{ag}}{t_{wg}}$ is change in transmittance of the glass window when it is operated in the water compare to air.

When Radiometer is submerged into other medium, Sensor's field of view becomes smaller and approximated by;

$$\Psi_m = \pi\theta_m^2 \tag{11}$$

Where, Ψ_m is the Sensor's viewing angle and θ_m is the half angle for the sensor.

According to Snell's Law when light passes form one medium to another medium [18],

$$\frac{\sin\theta}{\sin\theta'} = \frac{n'}{n} \tag{12}$$

Where, θ is the angle incident ray makes with normal perpendicular to interface. And θ' is the angle refractive way makes with normal perpendicular to interface. n is the refractive index of the incident medium. And n' is the refractive index of the passing medium where light is being passed.

Above Equation can be written by using notations a for air and w for water.

$$\frac{\sin\theta_w}{\sin\theta_a} = \frac{n_a}{n_w} \tag{13}$$

For Smaller field of view and $n_a = 1$, Eq. (13) will be given as;

$$\frac{\theta_w}{\theta_a} = \frac{1}{n_w} \tag{14}$$

From Eq. (11) and Eq. (14) Law of Radiance (n_w^2) is given by

$$\frac{\Psi_a}{\Psi_w} = n_w^2 \tag{15}$$

According to Fresnel's Equation [7] for reflectance and transmittance, Transmittance of the given window is given by;

$$t_{mg} = 1 - \frac{(n_m - n_g)^2}{(n_m + n_g)^2} \tag{16}$$

Where t_{mg} is the transmittance of the sensor's window in given medium. n_m is the refractive index of the medium in which sensor is being operated. n_g is refractive index of the sensor's window.

Eq. (16) should be written for two mediums using notations a for air and w for water.

$$t_{ag} = 1 - \frac{(n_a - n_g)^2}{(n_a + n_g)^2} \tag{17}$$

$$t_{wg} = 1 - \frac{(n_w - n_g)^2}{(n_w + n_g)^2} \tag{18}$$

By taking ratios of Eq. (17) & (18)

$$\frac{t_{ag}}{t_{wg}} = \frac{\left(\left(n_a + n_g\right)^2 - \left(n_a - n_g\right)^2\right) * (n_w + n_g)^2}{\left(\left(n_w + n_g\right)^2 - \left(n_w - n_g\right)^2\right) * (n_a + n_g)^2}$$

It can be further simplified and written as;

$$\frac{t_{ag}}{t_{wg}} = \frac{n_a(n_w + n_g)^2}{n_w(n_a + n_g)^2} \tag{19}$$

$$\frac{t_{ag}}{t_{wg}} = \frac{(n_w + n_g)^2}{n_w(1 + n_g)^2} \tag{20}$$

Using Eq. (10), (15) and (20) Immersion Co efficient is defined as;

$$I_{f_m} = \frac{n_w(n_w + n_g)^2}{(1 + n_g)^2} \quad (21)$$

As Immersion co efficient is wavelength dependent it can be also denoted as [17];

$$I_{f_m}(\lambda) = \frac{n_w(\lambda)(n_w(\lambda) + n_g(\lambda))^2}{(1 + n_g(\lambda))^2} \quad (22)$$

Immersion co efficient is wavelength dependent. While calculating, IC, we need to consider refractive index of medium and sensor's window as wavelength dependent as well. According to Austin and Halikas [3], wavelength dependence for Water RI, $n_w(\lambda)$ can be approximated by

$$n_w(\lambda) = 1.3251 + \frac{6.6096}{\lambda - 137.1924} \quad (23)$$

Sensor's window glass is made of BK-7 Schott glass. Whose wavelength dependent refractive indices $n_g(\lambda)$ are obtained from data sheet. BK-7 glass is designed to operate in 330nm – 2100nm range.

3.2 Experimental Calculations

Radiometer is deployed in the water while operating in the field. Immersion co efficient from theoretical calculations should be applied to correct the radiometric data after measurements but it is very important if we can collect radiometric data with corrected immersion factors practically.

3.2.1 Setup

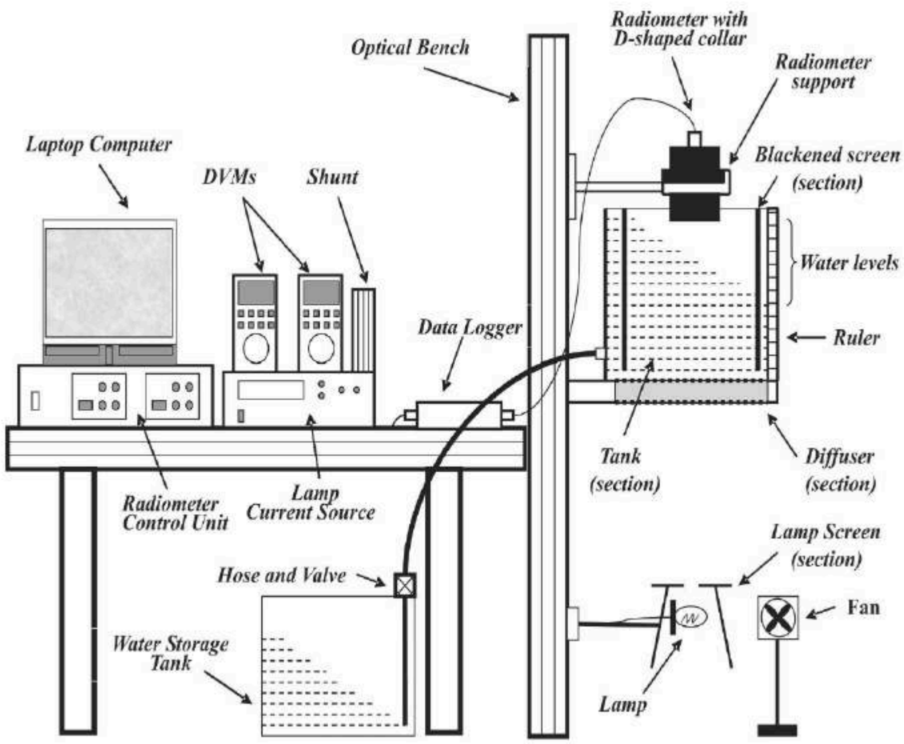

Figure 7 Setup for Immersion Experiment for calculations of Immersion co efficient of Radiometers [G. Zibordi, "Immersion Factor of In-Water Radiance Sensors: Assessment for a Class of Radiometers," *J. Atmos. Oceanic Technol.]*

In Fig. (7) Experimental setup is shown to calculate & characterize the immersion co efficient. Two tanks are shown in the figure where Storage tank is used to store the extra water while running the experiment and Main tank is used to measure the immersion data. Water is filled up at 30cm height in the main tank at the beginning where sensor window is just touching the water surface. Using the siphon and valve, water level is lowered 2cm at each measurement throughout experiment finishing at 2cm water level. 15 Measurements are taken starting from Water point (30cm) to in Air point (2cm).

Lamp [Light Source] is mounted at the bottom of main tank 25cm above bottom of the setup with a lamp cover located at 10cm above lamp. Three Diffusers are used at the bottom of the main tank to give uniform light visible to sensor.

Description	**Specification/ Value [cm]**
Floor – Lamp Distance	25
Storage Tank Size [H*W*L]	42*37*37
Main Tank Size [H*W*L]	37*34*34
Lamp – Lamp Cover Distance	10
Lamp – Diffuser Distance	75
Window – Diffuser top Distance	33
Diameter of Lamp Screen Aperture	5
Diameter of Visible Source [At Bottom of Main Tank]	30

Table 1 Specification and distances of various quantities in the experimental setup for immersion co efficient $\boldsymbol{I_{fm}}$ measurements.

3.2.2 Data Collection & Processing

Spectral radiance of radiometer in water is given by $DN_p(0^-)$ [In Water Measurements] in W S_r^{-1} m^{-2} Hz^{-1} when instrument is submerged in to water and taking measurements. Zi is the Distance from Sensor's window to the water surface as shown in figure below.

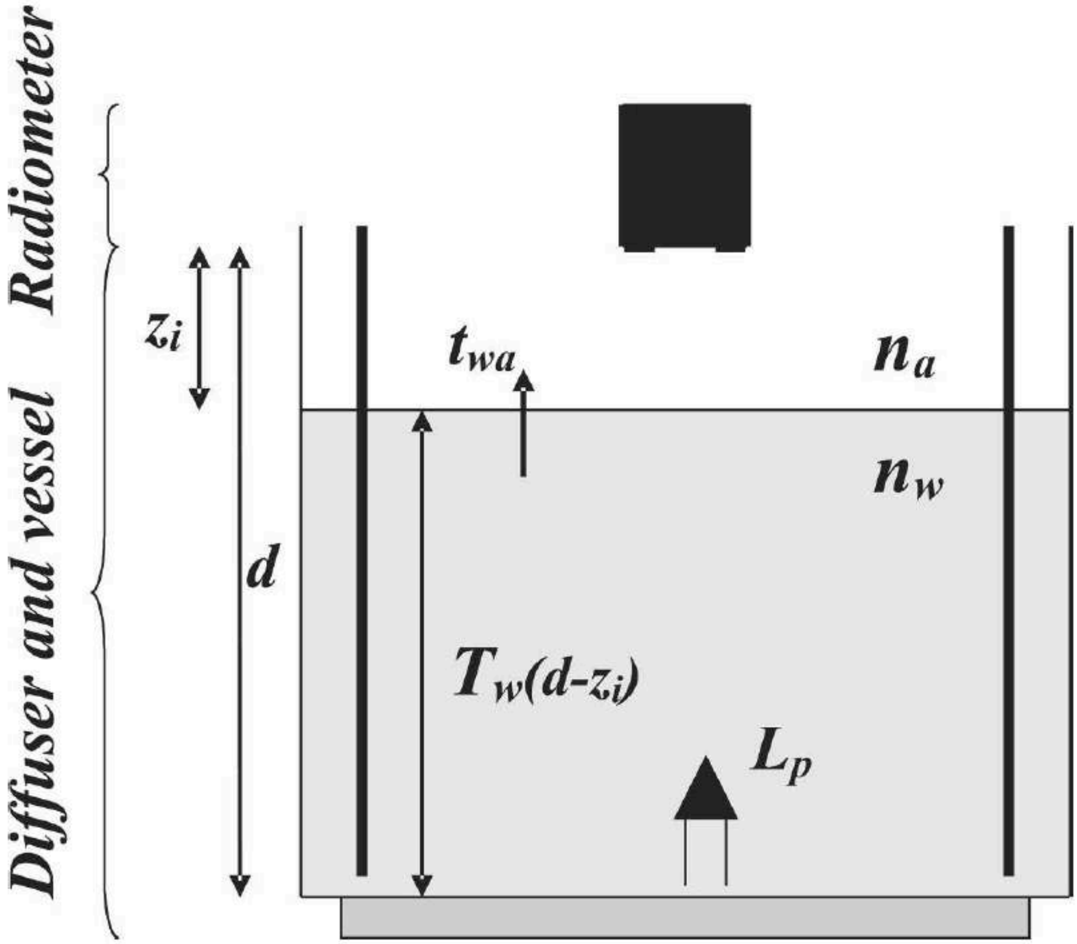

Figure 8 Diagram for various distances and quantities used in taking practical determination of $\boldsymbol{I_{f_w}}$ measurements. $\boldsymbol{L_p}$ Indicates Light Source located at the bottom of the tank.

$DN_p(0^+)$ represents in air measurements, if we take this measurement at z=0 then water touches the sensor's window and it will be in water measurement. $DN_p(0^+)$ is extrapolated by least square method to get to the point where water just touches the sensor's window. For any given wavelength, sensor's spectral radiance is denoted as function of Zi and is given by;

$$DN_p(i) = DN_p(d, z_i) \frac{T_w(d, 0)}{T_w(d, z_i)} \tag{24}$$

Where, $DN_p(d, z_i)$ is calculated from the data collected by radiometer at various distances ranging from 0cm to 30cm. Where d is the distance from bottom of the main tank to water surface as shown in Fig. (8). $d - z_i$ Is the depth of the water at given measurement visible from sensor's window. Transmittance $T_w(d, z_i)$ is given by;

$$T_w(d, z_i) = e^{-c(d - z_i)} \tag{25}$$

Where; c is spectral beam attenuation as a result of absorption and scattering effect. $DN_p(0^+)$ Measurements are taken in the experiment by lowering water level to 2cm each time starting from in water point $DN_p(0^-)$.

After collecting all 15 data points, From Eq. (7) and Eq. (10), I_{f_m} is determined by

$$I_{f_w} = \frac{DN_p(0^+)\Psi_a}{DN_p(0^-)\Psi_w t_{wa}} \tag{26}$$

Where, $\frac{\Psi_a}{\Psi_w}$ is change in sensor's field of view when it is submerged into water.

CHAPTER 4 EXPERIMENTS, RESULTS AND ANALYSIS

In this Chapter progress of experiments is shown and at end of each experiment, results are discussed and analysed. Based on the analysis and conclusions, modifications were done in experimental setup.

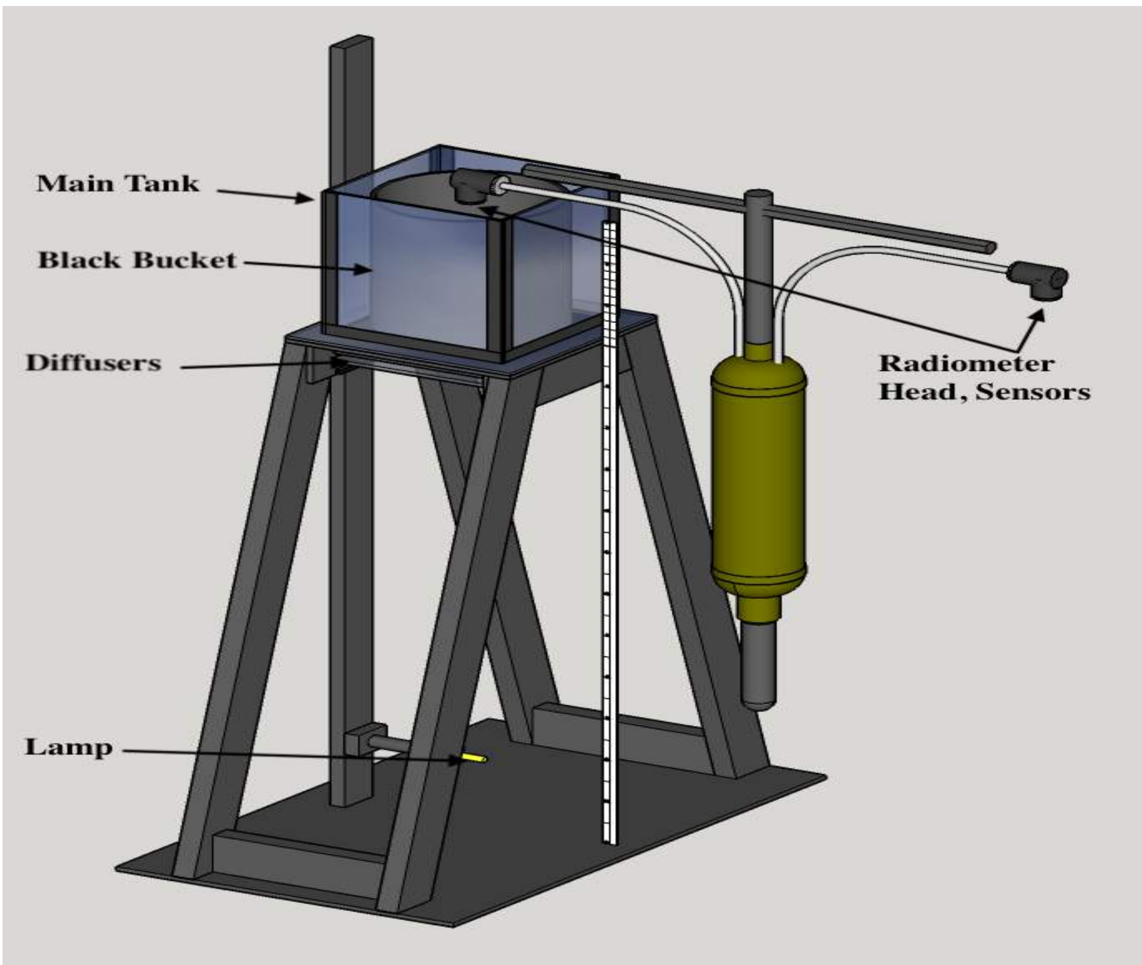

Figure 9 Experimental Setup with Basic component shown. Radiometer head is facing down, pointed at Light source.

3.1 HyperOCR 444 Radiance Sensor [256 Channel]

To determine the immersion co efficient of Radiometers, HyperOCR 444 was used in the initial experiments. HyperOCR 444 is radiance sensor. Actual experimental Laboratory setup is shown in the Figure below.

Figure 10 Actual Experiential lab setup while taking measurements with HyperOCR 444 Radiance sensor.

HyperOCR 444 was mounted on top of the main tank and tank was filled up to 30cm with tap water. Siphon and valve were used to lower the water level 2cm each time while taking measurements, finishing the one experiment at 2cm water level. Using HyperOCR 444 multiple experiments were carried out to determine Immersion co efficient practically and they were compared with theoretical values. Results for two of these experimental runs are shown in the figures below.

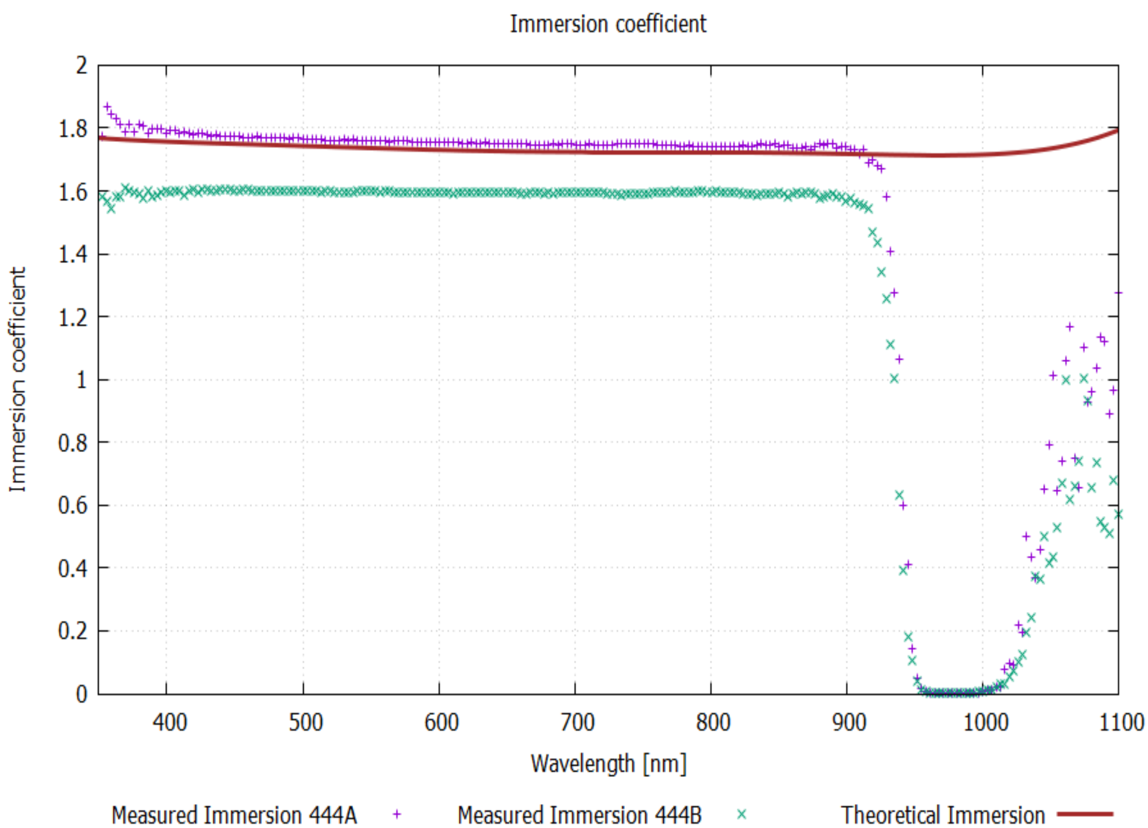

Figure 11 Plot for Measured and theoretically calculated Immersion Co efficient for HyperOCR 444 Radiance sensor.

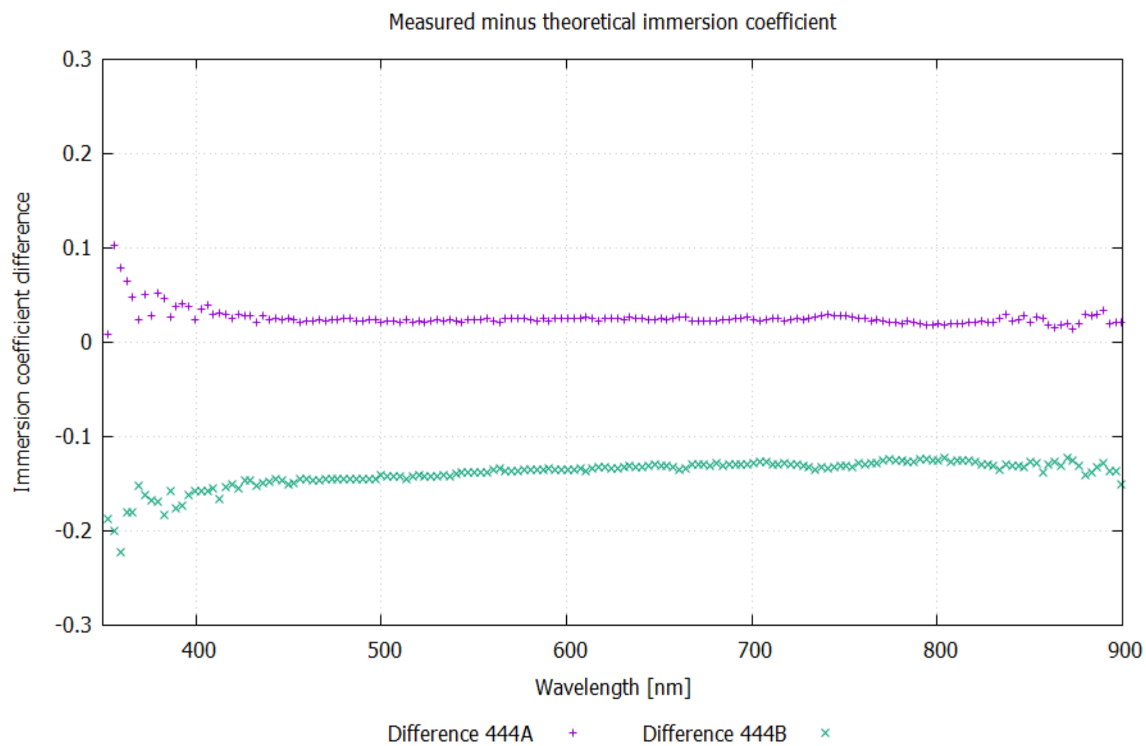

Figure 12 Plot for difference in Measured and theoretically calculated Immersion Co efficient for HyperOCR 444 Radiance sensor.

Analysis:

- At end of each experiment, main tank was filled up with water again from the storage tank using motor. And next experiment was carried out subsequently. So, there was not enough time given to water for settle down. Which have resulted in less light compare to first experiment.
- As tank was filled up with motor from storage tank, few solid particle dusts were also added to main tank, which did have affected the measurements in subsequent experiments.

3.2 HyperOCR 191 Radiance Sensor [256 Channel]

Modifications:

- To avoid solid particle dust 5micron filter were installed in the next series of experiments between main tank and storage tank while refilling.
- 2 hours of time were kept between each experiment to let water settle.
- HyperOCR 191 In water radiance sensor was used in further experiments.

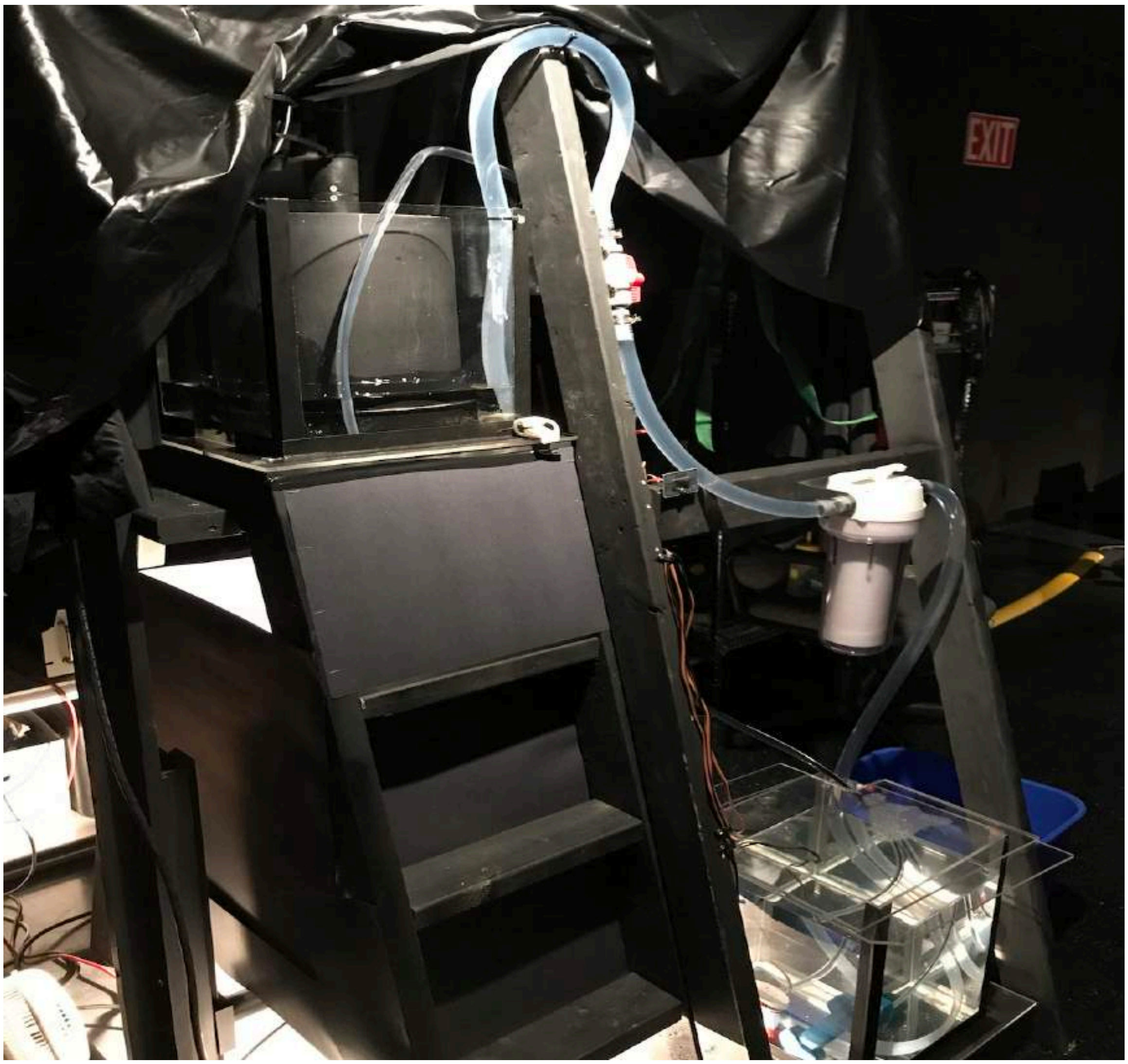

Figure 13 Modified Experiential lab setup with 5-micron filter while taking measurements with HyperOCR 191 Radiance sensor.

HyperOCR 191 was mounted on top of the main tank facing light source. 5-micron filter was used to filter the water while refilling. Using HyperOCR 191 multiple experiments were carried out to determine Immersion co efficient practically and they were compared with theoretical values. Results for two of these experimental runs are shown in figures below.

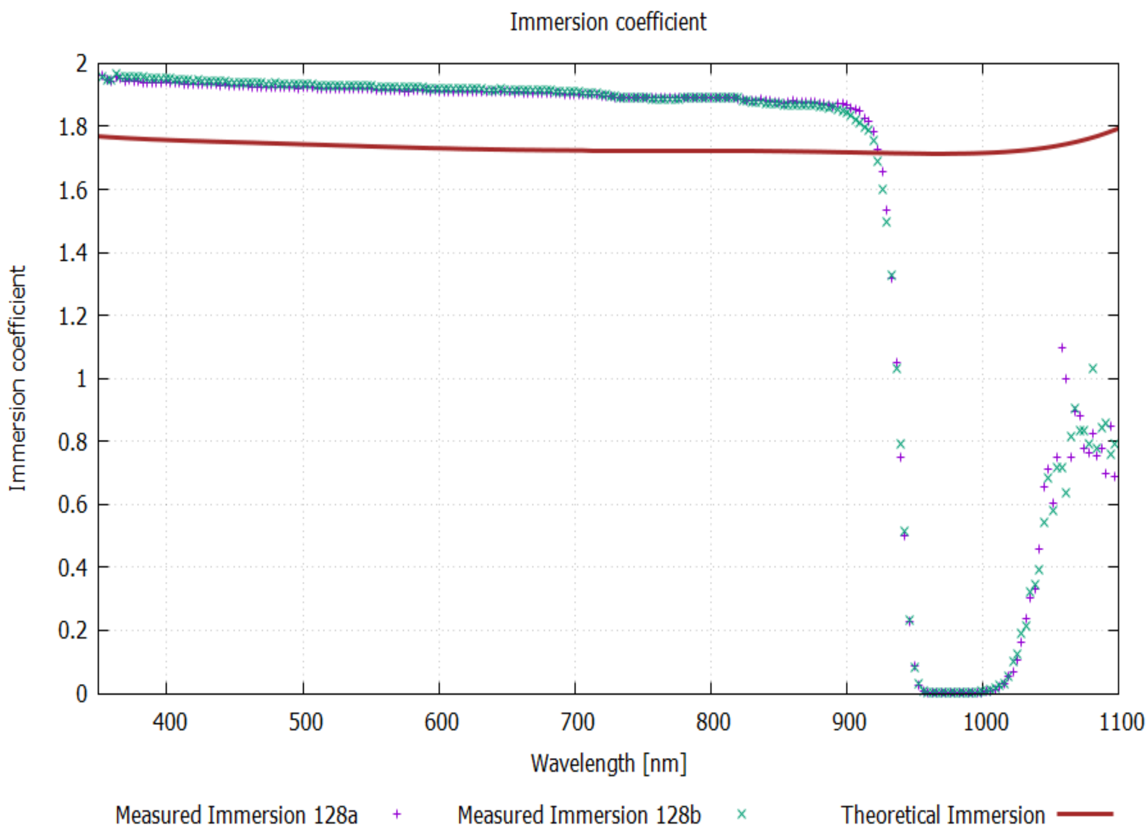

Figure 14 Plot for Measured and theoretically calculated Immersion Co efficient for HyperOCR 191 Radiance sensor.

Analysis:

- From Fig. (14) it was concluded that excellent repeatability was observed between two experiments and <1% data mismatching was observed.
- Results differ from theoretical calculation might be due to tap water and extra light added from the surroundings.

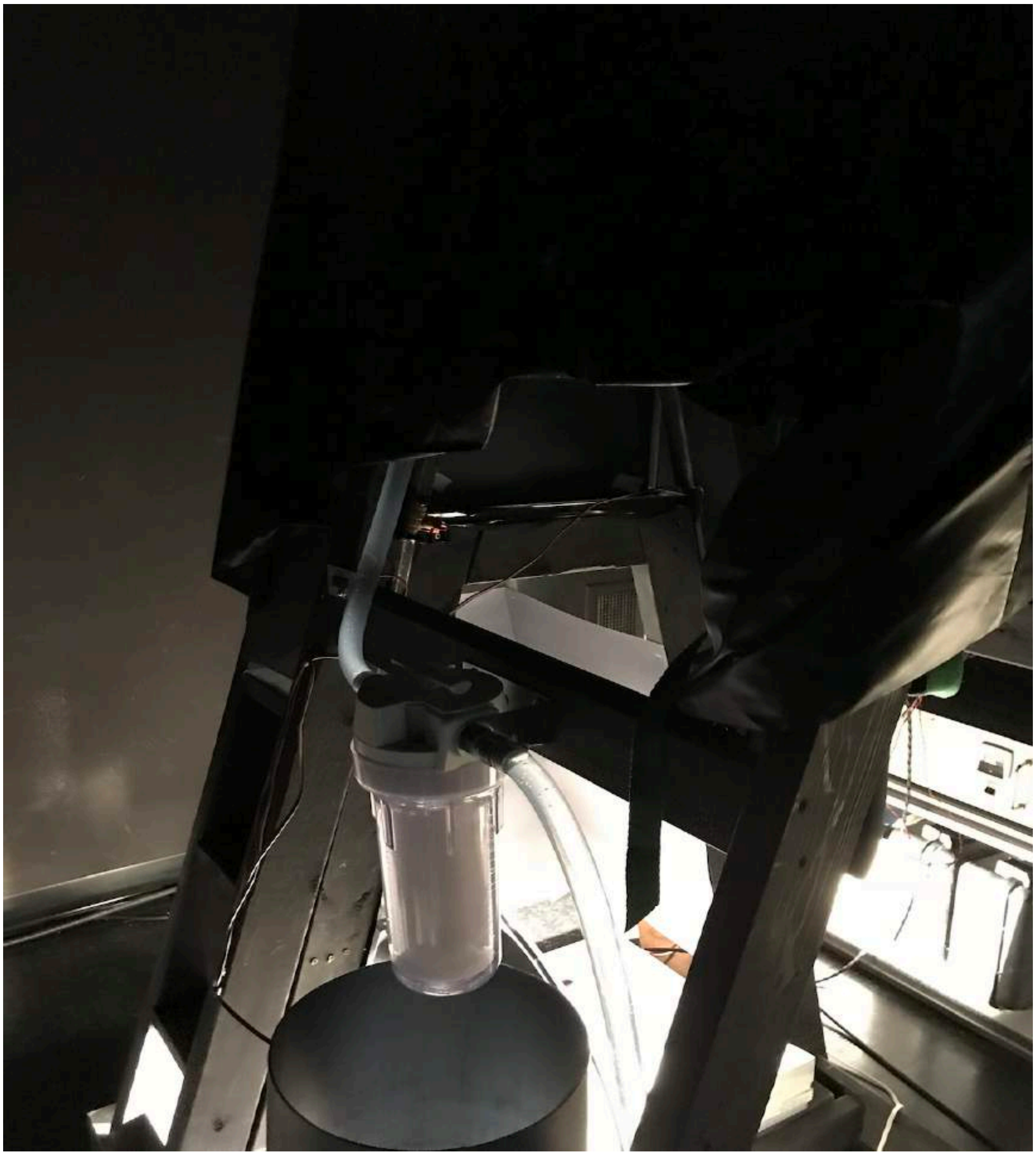

Figure 15 Modified experiential lab setup with tank cover to block extra lights from surroundings.

Modifications:

- Main tank was covered with additional black paper to block extra light from surroundings.
- Ultra pure water was used in subsequent experiments to achieve minimum discrepancy and maximum repeatability.

After all suggested modifications five experiments were carried out to determine Immersion Co efficient for HyperOCR 191 and results were plotted in the figure shown below.

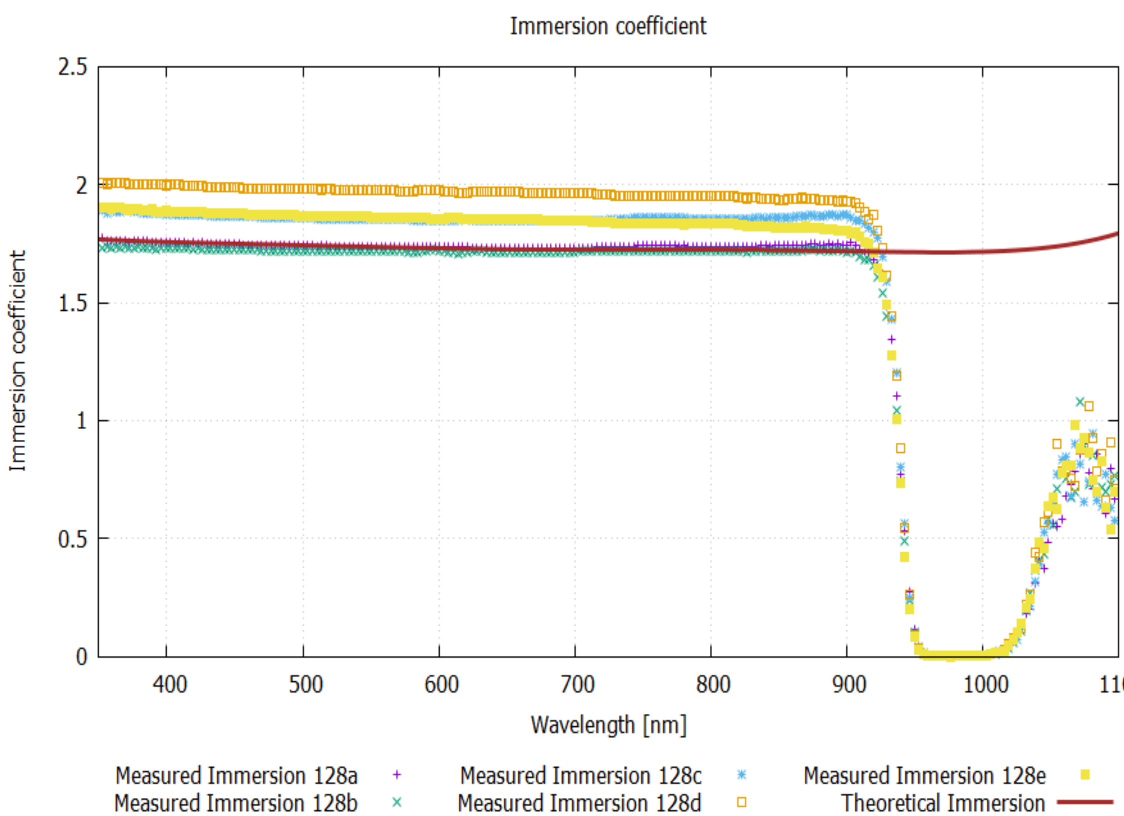

Figure 16 Plot for Measured and theoretically calculated Immersion Co efficient for HyperOCR 191 Radiance sensor after adding tank cover and ultra-pure water.

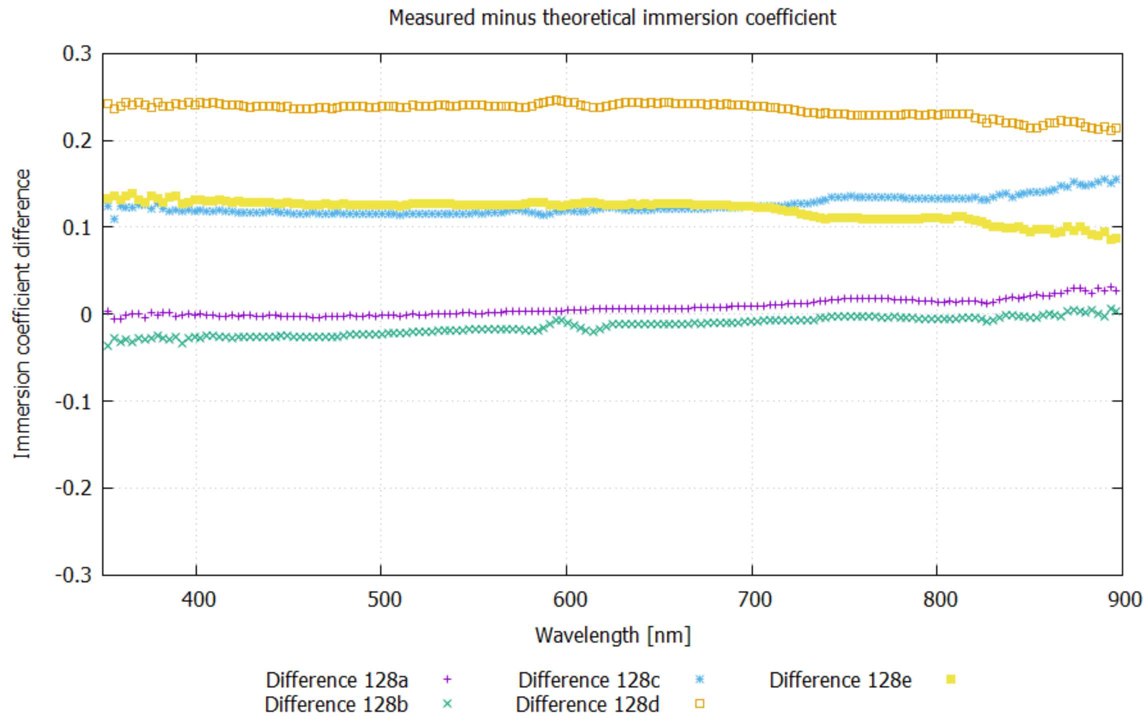

Figure 17 Plot for difference in measured and theoretically calculated Immersion Co efficient for HyperOCR 191 Radiance sensor for five sub sequent runs.

Analysis & Modification:

- From Fig. (17) it was concluded that experimental repeatability was poor that might have resulted from poor light distribution from lamp. So, lamp cover was designed as further modification, which will be mounted on post at 10cm from the lamp.
- New bucket was designed to put inside the main tank to block extra light from surroundings.
- Lamp Stability was also monitored for the whole experiment using reference sensor HyperOCR 426 and it was plotted to monitor any deviation in the lamp intensity.

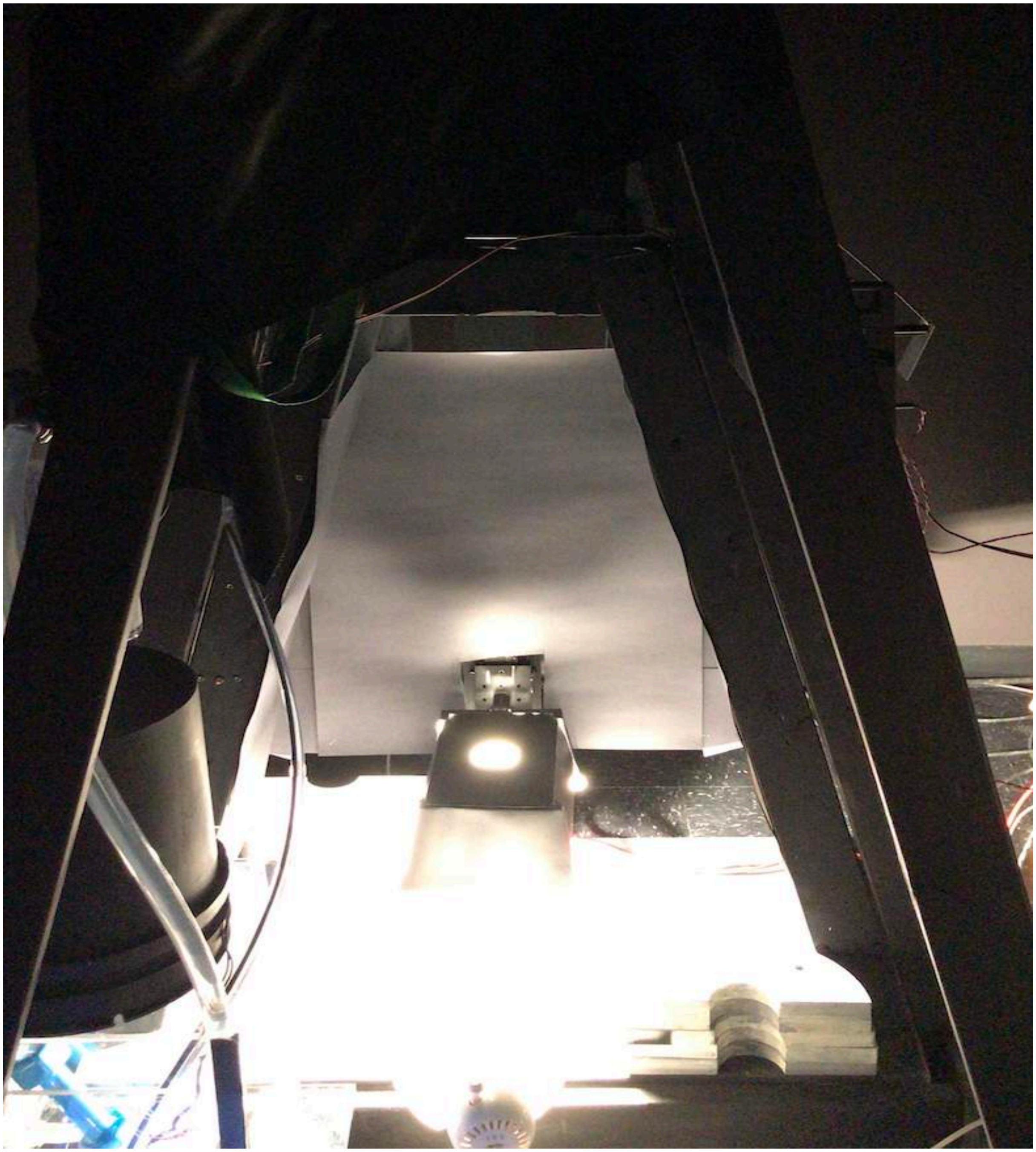

Figure 18 Lamp Cover to form light beam for uniform light distribution and to prevent reflections.

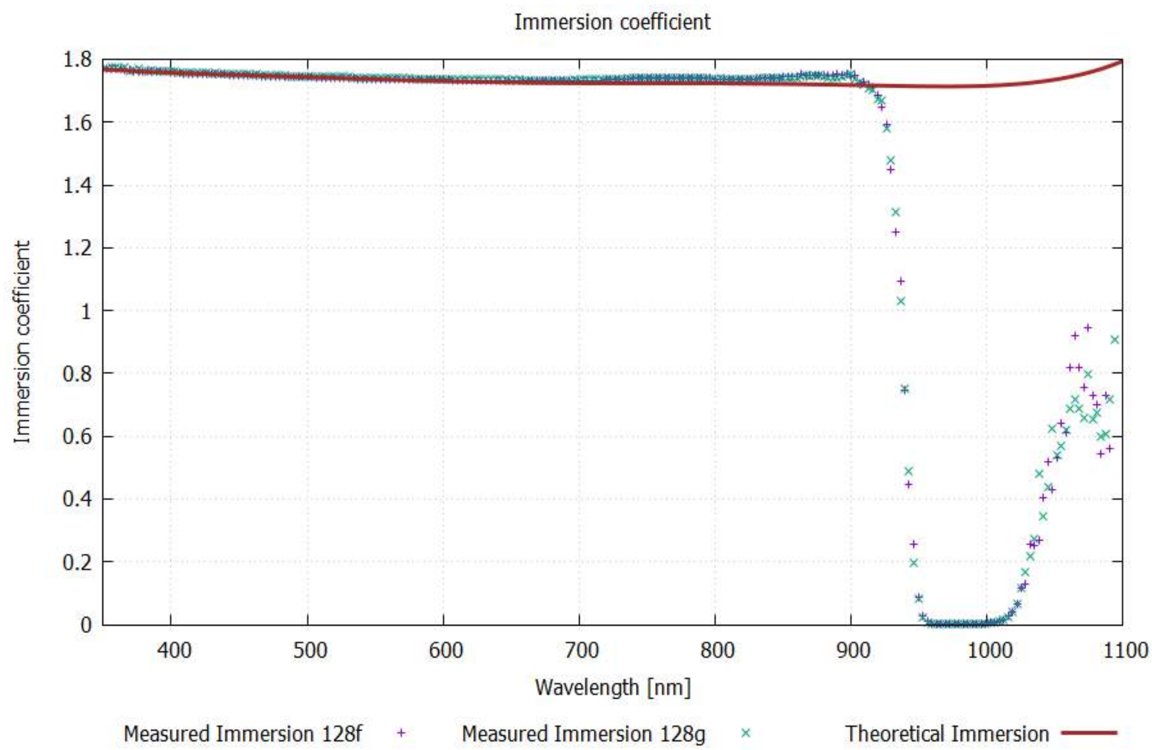

Figure 19 Measured and theoretically calculated Immersion Co efficient plotted for HyperOCR 191 Radiance sensor after adding new bucket and observed lamp stability.

4.2.1 Lamp Stability

Lamp stability is important factor to take into consideration while determining immersion co efficient. Each experiment takes about 2-3 hours to complete and during this period of time lamp must work as a stable source. NIST Calibrated 1000w FEL Lamp was used during experiments.

In the previous experiments, lamp stability wasn't observed, and it may have affected the results. Using HyperOCR 426 lamp stability was observed and plotted simultaneously while running an experiment.

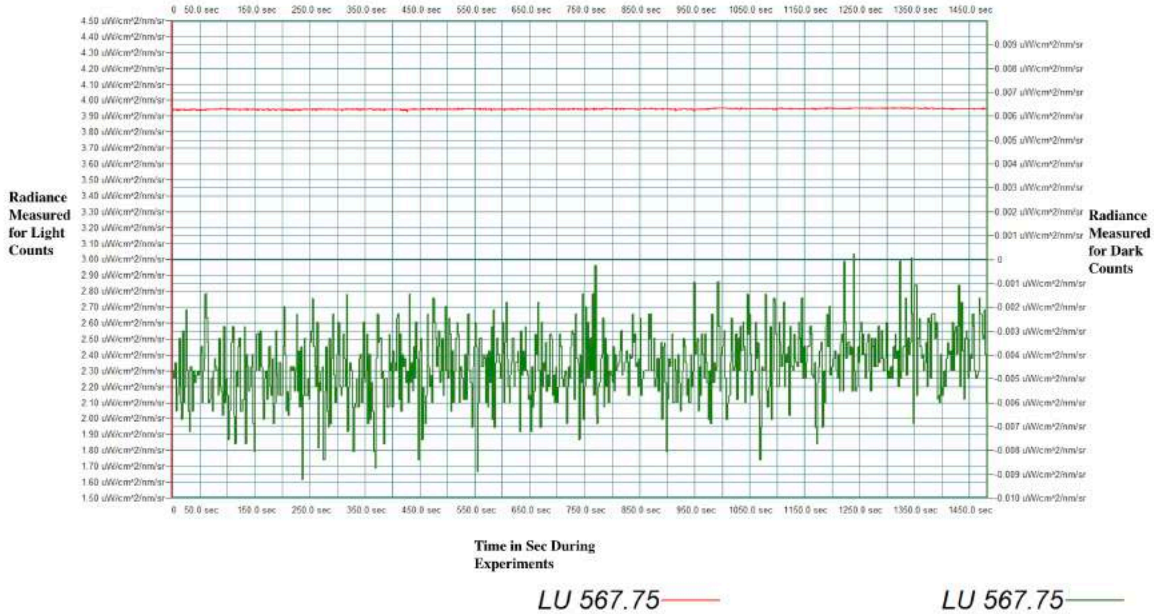

Figure 20 Light counts [Red] [Averaged] and Dark counts [Green] observed by HyperOCR 426 to monitor FEL Lamp Stability over the experiment.

Analysis:

- From Fig. (20), Y axis, On Left hand side of the plot, Radiance measurement for Light count is shown [Red curve][Averaged] and Y axis, On Right hand side of the plot, Radiance measurement for the Dark Count [Green Curve] is shown. By looking at the Red curve it was concluded that lamp was stable during the experiments for HyperOCR 191.
- To check the lamp stability HyperOCR 426 is mounted permanently for the subsequent runs.

Modification:

- To make experimental setup more stable, vernier scale was implemented to control distance between sensor's window and base of the tank.
- Tank level was checked at the base to make sure we are getting vertical half angle view and sensor is not tilted.

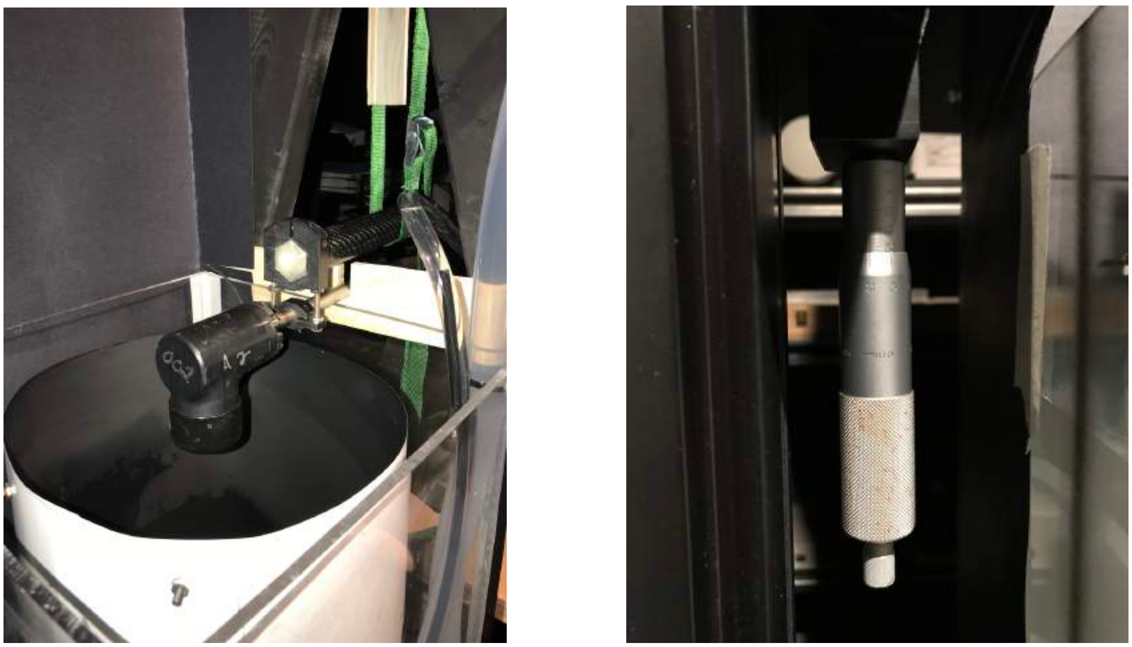

Figure 21 Sensor's window shown on left hand side. Vernier scale to set distance between sensor's window and Bottom of the tank.

After all suggested modifications five experiments were carried out to determine Immersion Co efficient for HyperOCR 191 and results were plotted in the figure shown below.

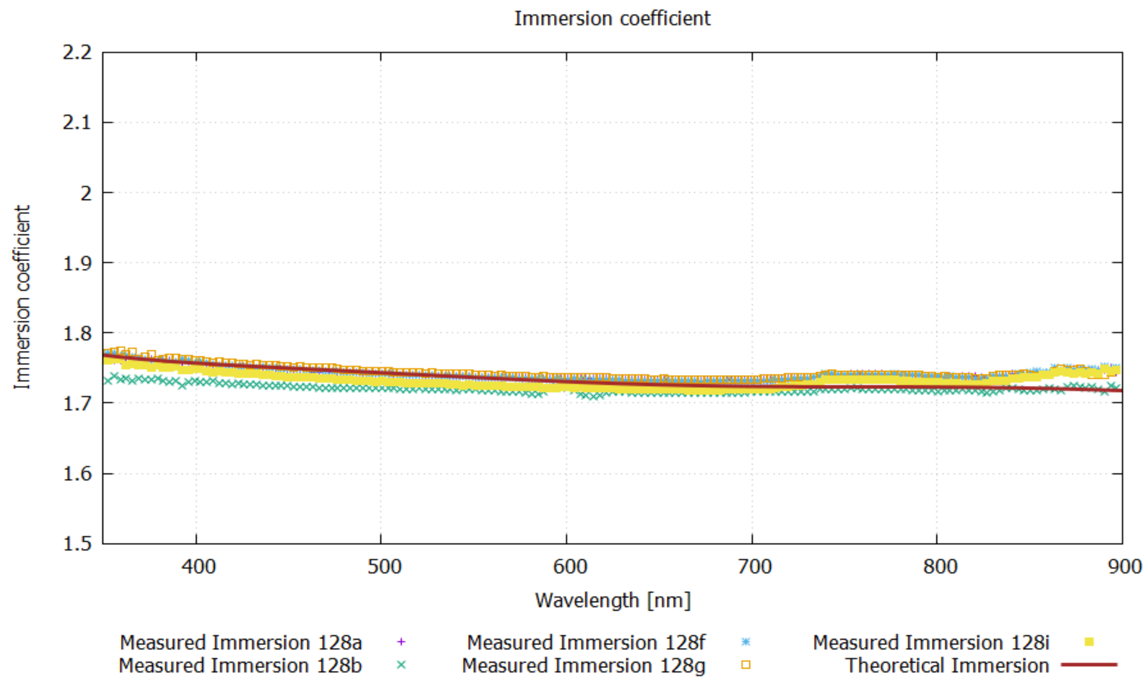

Figure 22 Measured and theoretically calculated Immersion Co efficient plotted for HyperOCR 191 Radiance sensor after adding vernier scale and tank stability.

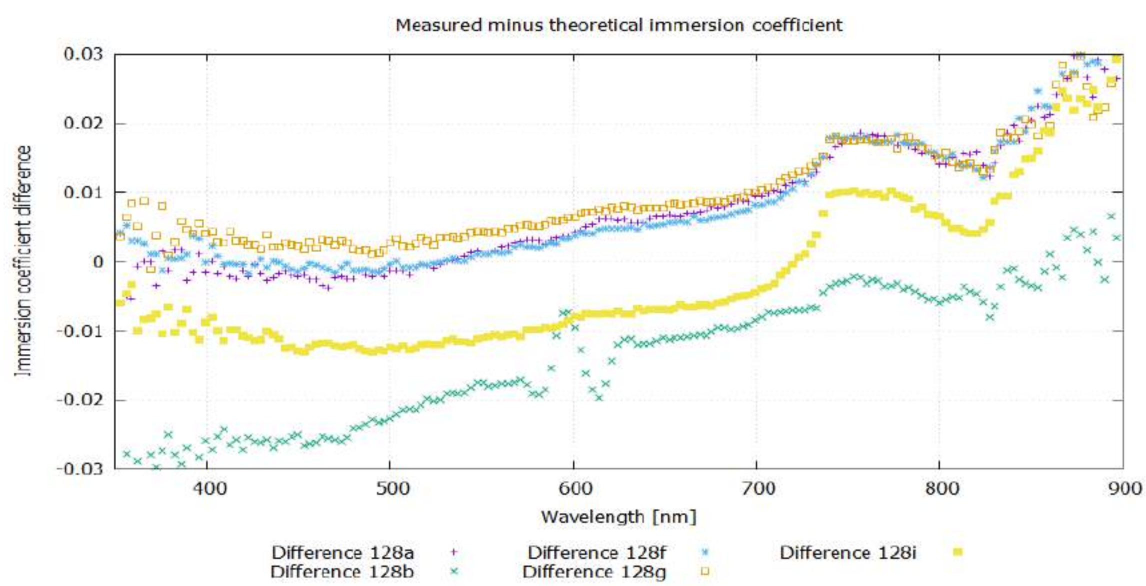

Figure 23 Plot for difference in measured and theoretically calculated Immersion Co efficient for HyperOCR 191 Radiance sensor.

3.2 HyperNav Radiance Sensor [2048 Channel]

Complete Experimental setup is shown in the figure below with all the previous modifications with HyperNav mounted in the setup.

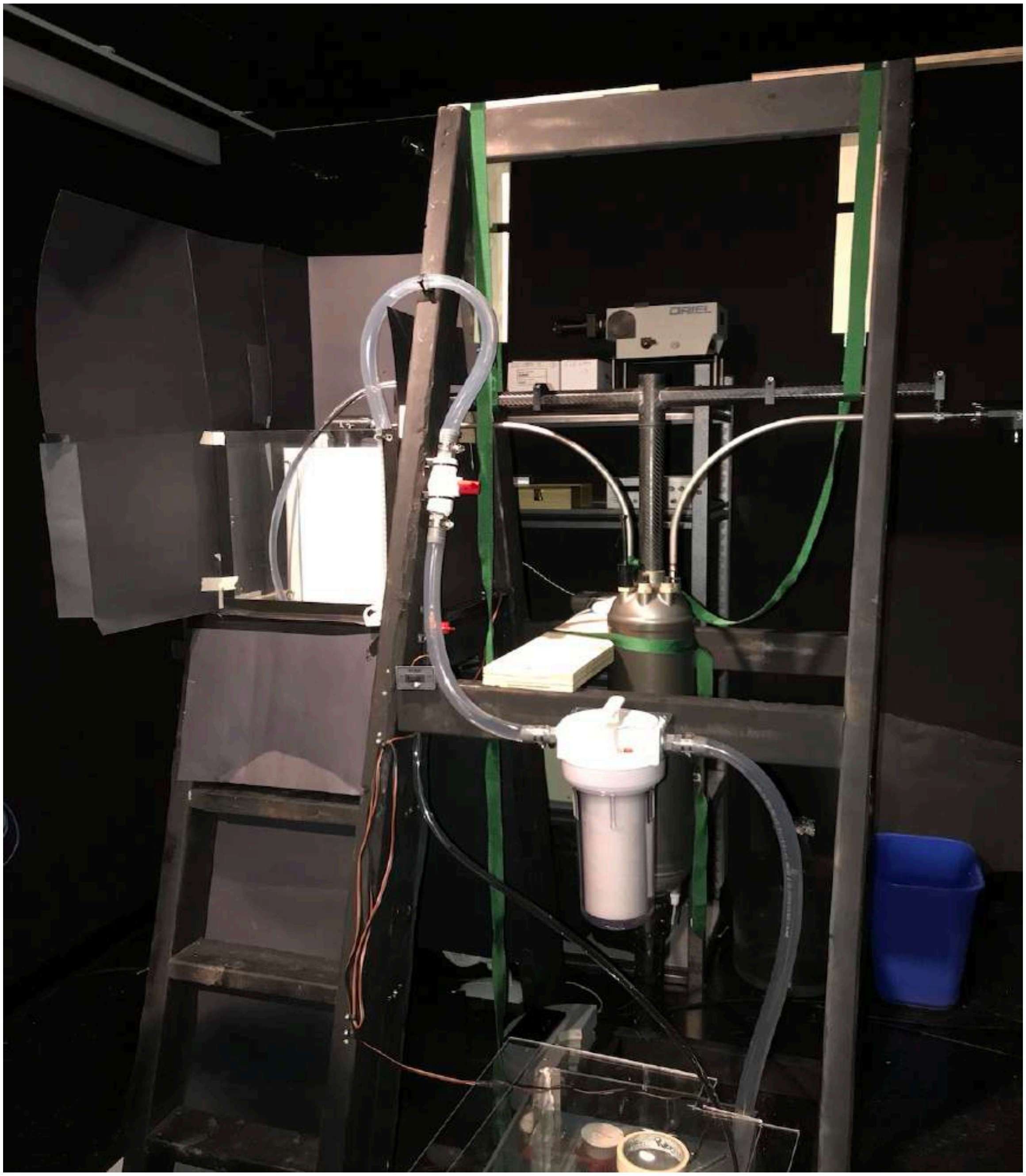

Figure 24 HyperNav Experimental setup to determine immersion co efficient.

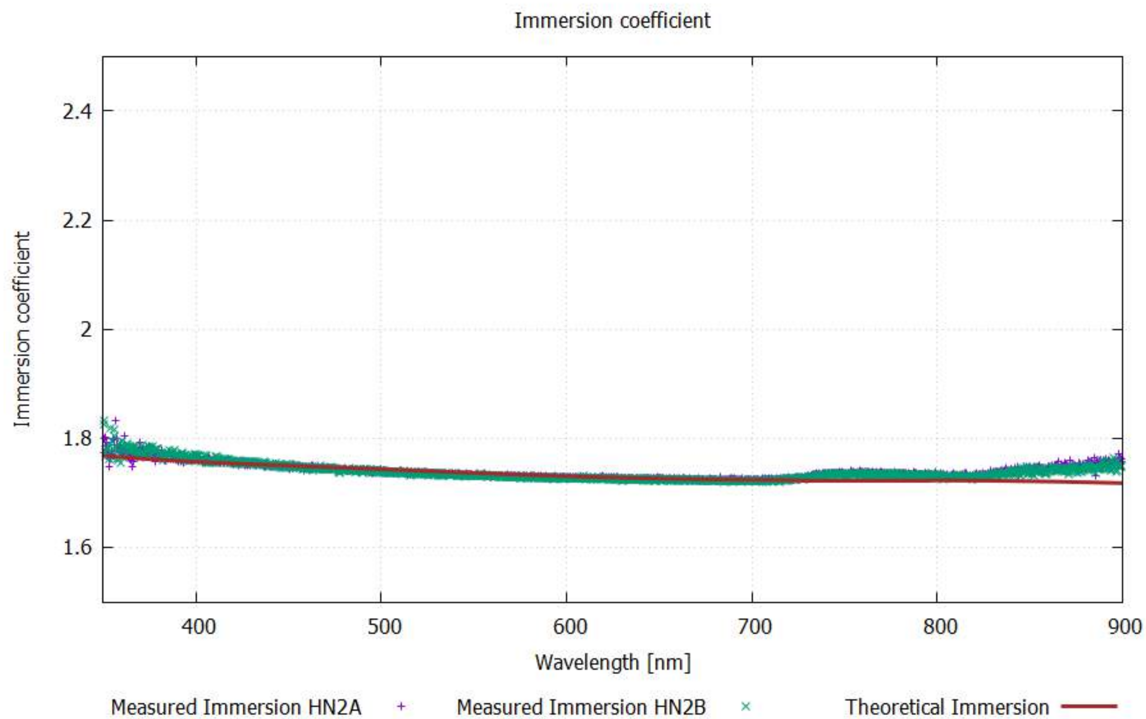

Figure 25 Measured and theoretically calculated Immersion Co efficient plotted for HyperNav Radiance sensor [2048 Channel] from 350-900nm.

Analysis:

- In Fig. (25) HyperNav System 1, Head 2 Data is shown for two experiments. Stray Light effect comes in to picture in near infrared region of the spectrum.
- Stray light is unwanted signal from the effect of reflection and scattering of the light. Sensor cannot differentiate between actual light and stray light. Stray light effect is high in UV and near Infrared region.

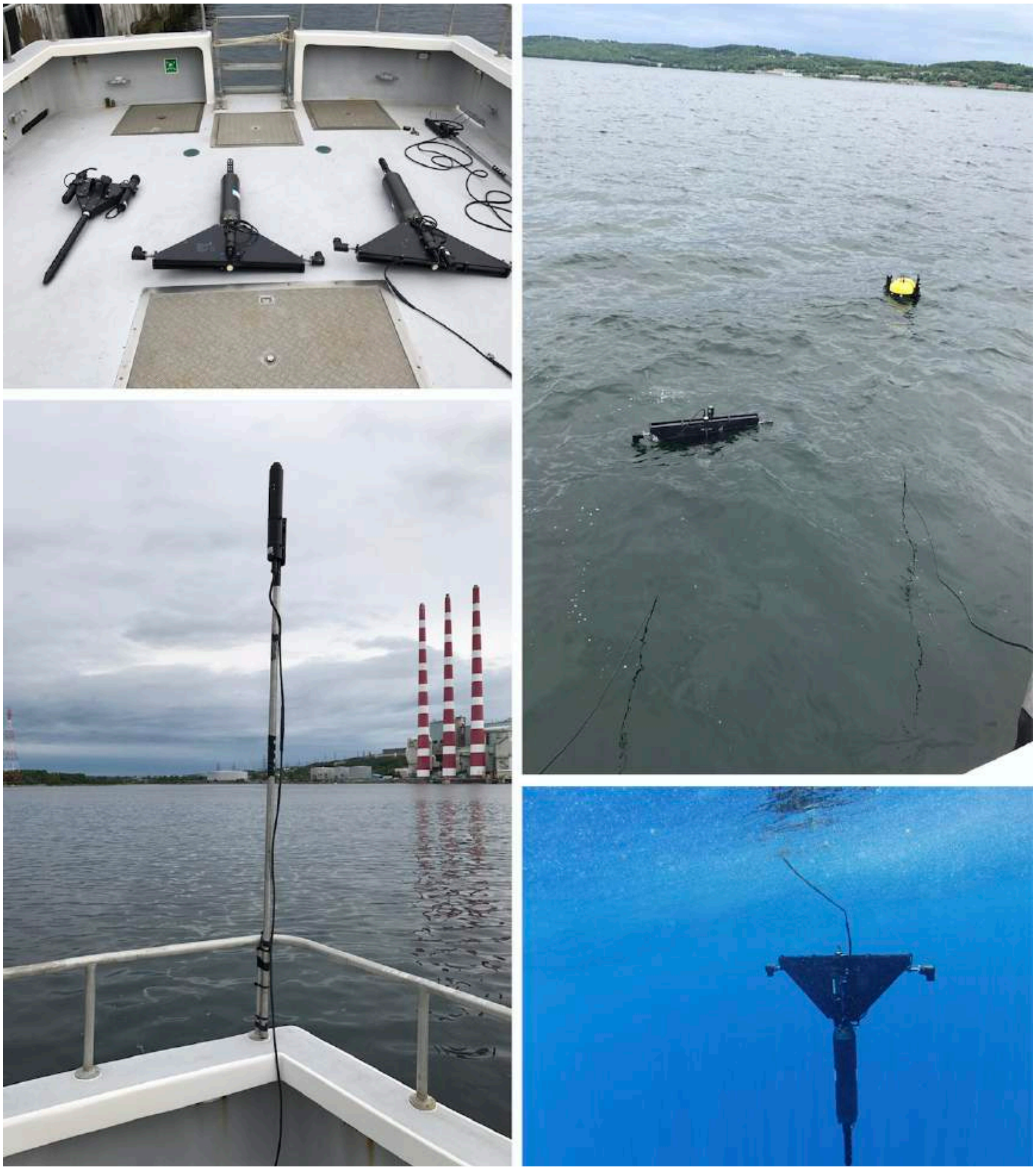

Figure 26 Field Experiment in Bedford basin with HyperNav System 1 and 3 shown in picture 1&2. Picture 3 is the reference sensor used to monitor sunlight. Picture 4 shows the deployment of HyperNav system 2 in the Hawaii.

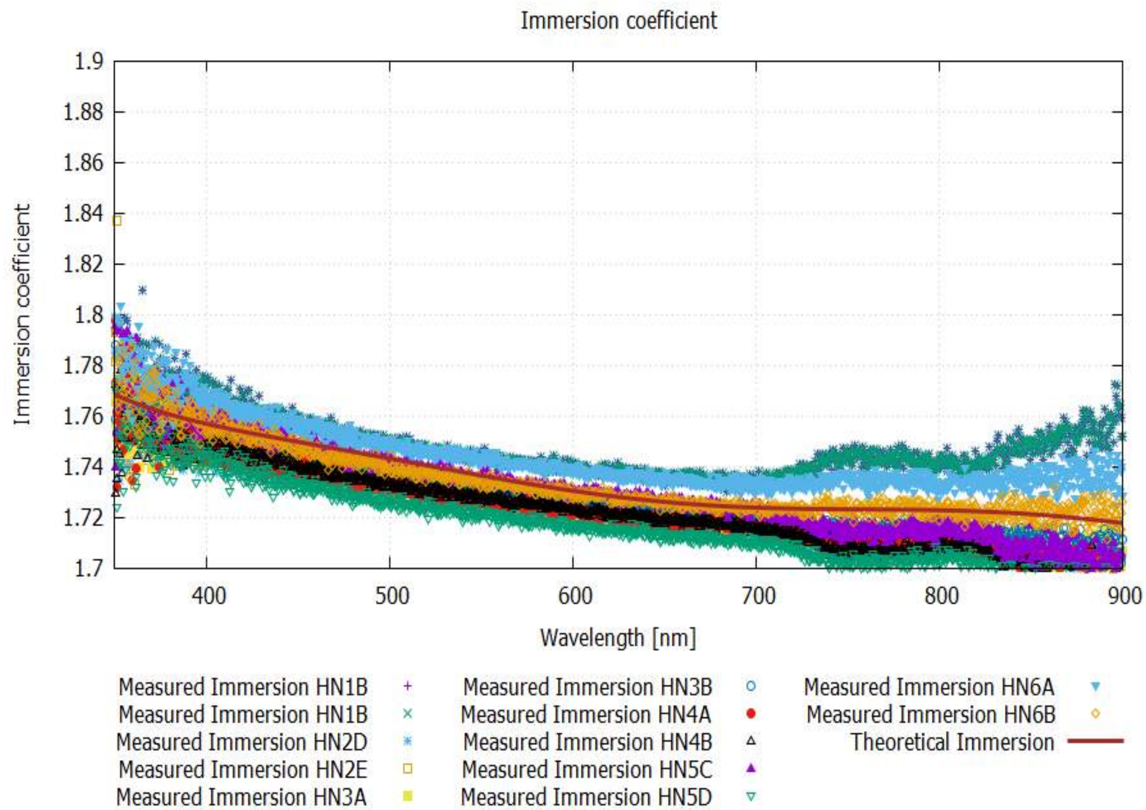

Figure 27 Measured and theoretically calculated Immersion Co efficient plotted for HyperNav Radiance sensor [2048 Channel] for all 3 systems and 6 sensors from 350-900nm.

CHAPTER 5 CONCLUSION

In this chapter, I have summarised the conclusion for the research carried out based on research objectives stated in Chapter 1.

5.1 My Contribution

- Immersion co efficient were theoretically calculated based on the model described in Chapter 3 and also practically determined from the lab experimental setup with various Hyper spectral radiometers HyperOCR 444 [256 Channel], HyperOCR 191 [256 Channel] and HyperNav [2048 Channel]. HyperNav is the prototype float currently in development, which is going to be used for calibration of NASA's PACE satellite.
- Immersion co-efficient were calculated and measured for the full spectrum range, UV [350-400nm], Visible [400-700nm] and Near Infrared [700-900nm], Which is also PACE's operating spectrum range.

5.2 Conclusion

- Immersion co efficient are sensitive to stray light and extra light that is added from surroundings. Only precisely completed experiment gives the results that are closer to actual.
- Immersion co efficient are also sensitive to change in lamp stability over the period of time. They are also dependent on glass window that is being used while making sensor's window.
- Theoretical and practically determined immersion co efficient differ <1% in Visible range [400-700nm] and <2% in near infrared regions.

- In nutshell, accuracy and repeatability of the experiments in determining immersion co efficient depends on the following factors.
    - Water being used while doing experiments.
    - Lamp Stability
    - Distance from where measurements are taken
    - Stray Light and Extra Light in the room.
    - Accuracy of the components used while designing experiment.

5.3 Recommendation for Setup

1. As the immersion coefficients depends on Lamp Stability, it is recommended to use the NIST calibrated FEL lamp while doing experiments.
2. Immersion coefficients are also sensitive to extra light being reflected and transmitted from objects present in the lab and also from the setup itself. So, it is advised to use non-reflective black curtain to cover the main tank. Also, Non-reflective round bucket inside the main tank while doing experiments.
3. Next factor to consider is the temperature. As Immersion coefficients are highly sensitive to temperature it is recommended to maintain a stable temperature while doing to experiments.
4. Accuracy, while lowering the water level, is also a critical factor. When water level is being lowered from 30cm to 2cm while doing experiments, at each measurement it is recommended to check if siphon is adding any more water after valve is closed. If it does then it will be a failed data point.
5. If tank is not balanced, sensor’s field of view is tilted, and it will not point at uniform light distribution, sensor will have less light to observe. So, it is also critical to have balanced tank setup.

5.4 Future Work

- During this research work, experimental setup was analysed and slowly modified after each experiment where many of the components used were hard to setup due to accuracy in distances. Lego parts can be used in future to design more robust and accurate setup which can be used for multiple sensors.

- Magenta filter can be used to explore sensor's response in ultraviolet and near infrared regions and to achieve more accurate results in Ultraviolet [350-400nm] and Near Infrared [700-900nm] regions.

BIBLIOGRAPHY

[1] E. Aas, "On submarine irradiance measurements," *Institute of Physical Oceanography, University of Copenhagen,* vol. 23, pp. plus tables and figures, 1969.

[2] W. R. G. Atkins and H. H. Poole, "The Photo-Electric Measurement of the Penetration of Light of Various Wave-Lengths into the Sea and the Physiological Bearing of the Results," *Philosophical Transactions of the Royal Society of London. Series B, Containing Papers of a Biological Character,* vol. 222, pp. 129-164, 1932.

[3] R. W. Austin and G. Halikas, "The index of refraction of seawater," *Scripps Institute of Oceanography,* vol. 76, *(1),* pp. 64, 1976.

[4] A. N. Bashkatov and E. A. Genina, "Water refractive index in dependence on temperature and wavelength: A simple approximation," in *Saratov Fall Meeting 2002: Optical Technologies in Biophysics and Medicine IV,* 2003, .

[5] S. W. Brown, G. P. Eppeldauer and K. R. Lykke, "Facility for spectral irradiance and radiance responsivity calibrations using uniform sources," *Appl. Opt.,* vol. 45, *(32),* pp. 8218-8237, 2006.

[6] R. Buckingham and K. Staenz, "Review of current and planned civilian space Hyperspectral sensors for EO," *Canadian Journal of Remote Sensing,* vol. 34, pp. S187-S197, 2008.

[7] E. Collett, "Field guide to polarization," SPIE press Bellingham, vol. 15, 2005.

[8] C. J. Donlon and G. Zibordi, "Chapter 3 - In Situ Optical Radiometry," *Experimental Methods in the Physical Sciences,* vol. 47, pp. 245-246, 2014.

[9] M. Feinholz *et al*, "Immersion Coefficients for the Marine Optical Buoy (MOBY) Radiance Collectors," *Journal of Research of the National Institute of Standards and Technology,* vol. 122, *(31),* 2017.

[10] L. Ferrato and K. Wayne Forsythe, *Comparing Hyperspectral and Multispectral Imagery for Land Classification of the Lower Don River, Toronto.* 20135. DOI: 10.5539/jgg.v5n1p92.

[11] M. Garbey and W. Shyy, "A least square extrapolation method for improving solution accuracy of PDE computations," *Journal of Computational Physics,* vol. 186, *(1),* pp. 1-23, 2003.

[12] A. Heidinger, C. Cao and J. T. Sullivan, "Using Moderate Resolution Imaging Spectrometer (MODIS) to calibrate advanced very high resolution radiometer reflectance channels," *Journal of Geophysical Research,* vol. 107, *(D23),* pp. AAC 11-1, 2002.

[13] Ø. Kleiv *et al*, "Estimation of upward radiances and reflectances at the surface of the sea from above-surface measurements," 2015.

[14] A. Morel, "Optical properties of pure water and pure sea water," *Optical Aspects of Oceanography,* vol. 1, *(1),* pp. 1-24, 1974.

[15] J. L. Mueller and R. Austin, "Characterization of oceanographic and atmospheric radiometers," *Ocean Optics Protocols for Satellite Ocean Color Sensor Validation, Revision,* vol. 4, pp. 17-33, 2003.

[16] J. L. Mueller and R. W. Austin, "Ocean optics protocols for SeaWiFS validation, revision 1," *Oceanographic Literature Review,* vol. 42, *(9),* pp. 805, 1995.

[17] T. Ohde and H. Siegel, "Derivation of immersion factors for the Hyperspectral TriOS radiance sensor," *Journal of Optics A: Pure and Applied Optics,* vol. 5, *(3),* pp. L12, 2003.

[18] C. Parazzoli *et al*, "Experimental verification and simulation of negative index of refraction using Snell's law," *Phys. Rev. Lett,* vol. 90, *(10),* pp. 107401, 2003.

[19] R. M. Pope and E. S. Fry, "Absorption spectrum (380–700 nm) of pure water. II. Integrating cavity measurements," *Appl. Opt.,* vol. 36, *(33),* pp. 8710-8723, 1997.

[20] R. Ramamoorthi and P. Hanrahan, "On the relationship between radiance and irradiance: determining the illumination from images of a convex Lambertian object," *J. Opt. Soc. Am. A,* vol. 18, *(10),* pp. 2448-2459, 2001.

[21] R. Smith, "An underwater spectral irradiance collector," *J. Mar. Res.,* vol. 27, *(3),* pp. 341, 1969.

[22] M. Soja-Woźniak *et al*, "Laboratory measurements of remote sensing reflectance of selected phytoplankton species from the Baltic Sea," *Oceanologia,* vol. 60, *(1),* pp. 86-96, 2018.

[23] K. J. Voss and S. Flora, "Spectral Dependence of the Seawater–Air Radiance Transmission Coefficient," *J. Atmos. Ocean. Technol.,* vol. 34, *(6),* pp. 1203-1205, 2017.

[24] K. J. Voss and d. C. Belmar, "Polarization properties of FEL lamps as applied to radiometric calibration," *Appl. Opt.,* vol. 55, *(31),* pp. 8829-8832, 2016.

[25] Werdell J. *PACE is NASA's Plankton, Aerosol, Cloud, ocean Ecosystem*. DOI: https://pace.oceansciences.org/about.htm.

[26] D. F. Westlake, "SOME PROBLEMS IN THE MEASUREMENT OF RADIATION UNDER WATER: A REVIEW," *Photochem. Photobiol.,* vol. 4, *(5),* pp. 849-868, 1965.

[27] W. L. Wolfe and G. J. Zissis, "The infrared handbook," *Arlington: Office of Naval Research, Department of the Navy, 1978, Edited by Wolfe, William L.; Zissis, George J.,* 1978.

[28] G. Zibordi, Donlon J. Craig and Parr Albert C., "In situ optical radiometry," in *Optical Radiometry for Ocean Climate Measurements*, Giuseppe Zibordi, Kenneth J. Voss, Ed. ScienceDirect, 2014, pp. 245-247.

[29] G. Zibordi and M. Darecki, "Immersion factors for the RAMSES series of hyper-spectral underwater radiometers," *Journal of Optics. A. Pure and Applied Optics,* vol. 8, *(3),* pp. 252, 2006.

[30] G. Zibordi *et al*, "Characterization of the Immersion Factor for a Series of In-Water Optical Radiometers," *J. Atmos. Oceanic Technol.,* vol. 21, *(3),* pp. 501-514, 2004.

[31] G. Zibordi, "Immersion Factor of In-Water Radiance Sensors: Assessment for a Class of Radiometers," *J. Atmos. Oceanic Technol.,* vol. 23, *(2),* pp. 302-313, 2006.

[32] G. Zibordi, M. Talone and L. Jankowski, "Response to Temperature of a Class of In Situ Hyperspectral Radiometers," *Journal of Atmospheric & Oceanic Technology,* vol. 34, *(8),* pp. 1795-1805, 2017.

[33] S. Dobretsov, H. Dahms and P. Qian, "Inhibition of biofouling by marine microorganisms and their metabolites," *Biofouling,* vol. 22, *(1),* pp. 43-54, 2006.